$$U^{n+1}_{i,j,k} = U^n_{i,j,k} - \Delta t L(U^n_{i,j,k}),$$

where $\Delta t = t^{n+1} - t^n$ and L is

$$L(U_{i,j,k}) = \frac{\tilde{F}_{i+1/2,j,k} - \tilde{F}_{i-1/2,j,k}}{\Delta x_i} + \frac{\tilde{G}_{i,j+1/2,k} - \tilde{G}_{i,j-1/2,k}}{\Delta y_j}$$
$$+ \frac{\tilde{H}_{i,j,k+1/2} - \tilde{H}_{i,j,k-1/2}}{\Delta z_k} + S_{i,j,k}$$

Fluxes along each direction, for example x, was defined by local-characteristic method [1] as follows

$$\tilde{F}_{i+1/2,j,k} = \frac{1}{2}\left[F_{i,j,k} + F_{i+1,j,k} + R_{i+1/2}W_{i+1/2}\right]$$

where $R_{i+1/2}$ is matrix right eigenvectors of Jacobian matrix $A(U) = \partial F/\partial U$.
The elements l of vectors $W_{i+1/2}$ is

$$(\phi^l_{i+1/2})^U = \frac{1}{2}\psi(a^l_{i+1/2})(g^l_{i+1} + g^l_i) - \psi(a^l_{i+1/2} + \gamma^l_{i+1/2})\alpha^l_{i+1/2}$$

where

$$\gamma^l_{i+1/2} = \frac{1}{2}\psi(a^l_{i+1/2})\begin{cases} (g^l_{i+1} - g^l_i)/\alpha^l_{i+1/2} & ,\alpha^l_{i+1/2} \neq 0 \\ 0 & ,\alpha^l_{i+1/2} = 0 \end{cases}$$

The amplitude of waves $\alpha^l_{i+1/2}$ is elements of vectors

$$\alpha_{i+1/2} = R^{-1}_{i+1/2}(U_{i+1,j,k} - U_{i,j,k}).$$

The function ψ is

$$\psi(z) = \begin{cases} |z| & ,|z| \geq \delta_1 \\ (z^2 + \delta_1^2)/2\delta_1 & ,|z| < \delta_1 \end{cases}$$

and define entropy correction by $|z|$, where δ_1-small positive parameter. The function-limiter g^l_i was defined as follows:

$$g^l_i = minmod(\alpha^l_{i-1/2}, \alpha^l_{i+1/2})$$

$$g^l_i = (\alpha^l_{i+1/2}\alpha^l_{i-1/2} + |\alpha^l_{i+1/2}\alpha^l_{i-1/2}|)/(\alpha^l_{i+1/2} + \alpha^l_{i-1/2})$$

The one step of time integration is defined by Runge-Kutta method [2] as

$$U^{(1)} = U^n + \Delta t L(U^n)$$
$$U^{(2)} = \frac{3}{4}U^n + \frac{1}{4}U^{(1)} + \frac{1}{4}\Delta t L(U^{(1)})$$
$$U^{n+1} = \frac{1}{3}U^n + \frac{2}{3}U^{(2)} + \frac{2}{3}\Delta t L(U^{(2)})$$

The time step is restricted to satisfy the Courant condition along each row in three directions, and is calculated with

$$\Delta t = CFL \times min\left(\frac{\Delta x}{|v_x| + c_s}, \frac{\Delta y}{|v_y| + c_s}, \frac{\Delta z}{|v_z| + c_s}\right)$$

and $CFL = 0.2$ typically. v_x,v_y,v_z are the velocity of matter in each direction and c_s is the speed of sound.
For higher resolution in the numerical modelling we have used three level of nested rectangular grids with 128 cells in each directions. Solution results for above described problem were obtained due to the NORMA system application [3] on the system with distributed memory multiprocesseres (two Alpha 21264/667 MHz in node, memory 1 Gb in node, SAN Myrinet

to communication, 384 nodes). Norma program was compiled in Fortran with MPI library. The speedup of computation in 122.8 times on 128 processors were obtained during solution process.
The evolution of entropy distributions are shown in figure 1 and 2. Two cross sections of the star are chosen as images. In the first cross section (fig.1), the horizontal axis corresponds to the x axis, while the vertical axes corresponds to the z axis of our coordinate system. The second cross section(fig.2) correspond to a view from above onto the plane of rotation, corresponding to the plane of the equator. The initial configuration is chosen at time t=0.075 ms, and the final configuration is shown for time t=6.31 ms. The complete evolution lasted 20 ms.
The two bubbles initially appear (at about 3 ms), elongated in opposite directions along the axis of rotation. Four additional bubbles appear soon afterwards (at about 5 ms) and lie in the plane of rotation of the protoneutron star. The bubbles located along the axis of rotation broken off the hot core first and float to the surface. This occurs because the density varies more rapidly along the axis of rotation. The bubbles located in the plane of rotation broken off the hot nucleus core later and also float to the surface. Our calculations show that, following the first bubbles, additional bubbles with significantly less volume are formed, which also begin to float to the surface.
The first stage of the development of the peturbations is the growth of asymmetry along the axis of rotation of the star, which lasts for 3 ms. The asymmetry is still very weakly expressed in the plane of rotation, and the evolution proceeds peacefully. The asymmetry of the distribution of the substance is negligible during this stage, and bubbles of hot matter have not yet been formed. In the next millisecond bubbles moving along the axis of rotation have already been formed and bubbles in the plane of rotation begin to be distinguished at this stage. On the last stage to the moment time 6 ms take place final formation of bubbles in the plane of the equator and motion their to the surface neutrinosphere. The bubbles along the axis of rotation have already escaped from the calculated region.
Figure 3 shows the three-dimensional profile of the entropy distribution initially (t=0.075 ms) and when the bubbles have already formed (t=3.65 ms). Figure 4 shows velocity field distribution, convective cells are clearly visible that show both the rise of hot matter to the surface and the fall of cold matter to the center of the protoneutron star.
The calculations showed that at a distance corresponding to the maximum gravity, a large scale bubble with a radius $\sim 2.0 \cdot 10^6$cm, density $\sim 4.0 \cdot 10^{11}$ g/cm^3 and temperature $\sim 5.0 \cdot 10^9$K emerges. The mass of one dredged-up element is $0.02 M_\odot$. The calculations indicated that the neutrino-rich matter reached density of $\sim 10^{11}$g/cm^3 in $\sim 10^{-2}$s, implying that the neutrinos contained in the matter freely escape from it in the regime of volume radiation. The shock from the initial bounce when the collapse in the stellar core stops will then be supported by the neutrino emission, resulting in the ejection of an envelope. Les us now estimate the intensity of the netrino emission. At the initial time, the mass of matter with entropy excess ($S_{max} = 1.4$) is $0.07 M_\odot$. In 4 ms, $0.02 M_\odot$ of this matter enters the region of densities lower than $\sim 10^{11}$g/cm^3, and the matter becomes transparent for the neutrinos in it. The number of these neutrinos is comparable to the number of electrons with a mean energy 30Mev. The intensity of the neutrino emission is $\sim 2.5 \cdot 10^{52}$ erg/s. The fraction of the energy of this neutrino emission absorbed by the matter per gram in shock is $\sim 2.0 \cdot 10^{24}$ erg/g s. This value is comparable to the neutrino losses from the shock front, i.e., the mechanism of explosive convection could support the diverging shock and lead to the ejection of a supernova envelope[4].

References

[1] Yee H.C., Klopfer G.H., Montagne J.L., JCP, **88**, p.31, 1990.

[2] Shu C.W., Osher S., JCP, **77**, p.439, 1988.

[3] A.N.Andrianov, K.N.Efimkin, V.Y.Levashov, I.N.Shishkova., Lecture Notes in Computer Science, v.2073, July, 2001.

[4] Ustyugov S.D., Chechetkin V.M., Astronomy Reports, **43**, p.718, 1999

Adaptive Discontinuous Galerkin Finite Element Methods for Nonlinear Hyperbolic Conservation Laws

Ralf Hartmann

University of Heidelberg, Germany

Multi-dimensional compressible fluid flows are modeled by nonlinear conservation laws whose solutions exhibit a wide range of localized structures, such as shock waves, contact discontinuities and boundary layers. The accurate numerical resolution of these features necessitates the use of locally refined, adaptive computational meshes. A majority of adaptive algorithms used to model compressible fluid flows will simply refine or adjust the computational grid according to an *ad hoc* criterion, such as a large gradient in a physical quantity or residual information, for example. Although this intuitive approach has had some success, it does not provide practical or sharp error estimation. Moreover, *ad hoc* refinement strategies may not provide the most economical mesh design for the control of a given error quantity of interest, cf. [2, 3, 4, 5], for example.

Given a bounded domain Ω in $\mathbf{R}^n$, $n \geq 1$, with boundary $\partial\Omega$, we consider the following problem: find $u : \Omega \to \mathbf{R}^m$, $m \geq 1$, such that

$$\nabla \cdot F(u) = 0 \quad \text{in } \Omega, \tag{1}$$

where, $F : \mathbf{R}^m \to \mathbf{R}^{m\times n}$ is continuously differentiable. An example of such a model problem is represented by the Euler equations of compressible gas dynamics.

The discontinuous Galerkin finite element method for (1) is defined as follows: find $u_h \in V_h^p$ such that

$$\sum_{K\in\mathbf{T}_h} \{-(F(u_h)\cdot\nabla v_h\,dx)_K + (H(u_h,\hat{u}_h,n)\,v_h)_{\partial K}\} = 0 \quad \forall v_h \in V_h^p, \tag{2}$$

or in short notation: find $u_h \in V_h^p$ such that

$$a(u_h, v_h) = 0 \quad \forall v_h \in V_h^p, \tag{3}$$

where $a(\cdot,\cdot)$ denotes the semi-linear form given by the left hand side of (2). Here, V_h^p denotes the finite element space consisting of discontinuous vector–(of dimension m)–valued polynomial functions of degree $p \geq 0$. Furthermore $H(\cdot,\cdot,\cdot)$ denotes a consistent and conservative *numerical flux* function, and $u_h|_{\partial K}$ and $\hat{u}_h|_{\partial K}$ denote the interior and outer traces of u_h on ∂K, respectively, whereas at the boundary $\partial\Omega$ $\hat{u}_h$ represents an appropriate boundary function. Furthermore, at curved boundaries a higher order boundary approximations is employed to avoid non-physical entropy production at reflective boundaries, see [1] for more details.

Inserting the exact solution u into (2) and using the consistency of the numerical flux function we deduce the consistency condition $a(u, v_h) = 0, \forall v_h \in V_h^p$. Thereby, following *Galerkin orthogonality* property of the finite element method (2) holds:

$$a(u, v_h) - a(u_h, v_h) = 0 \quad \forall v_h \in V_h^p. \tag{4}$$

This can be written in short notation

$$L(u, u_h; e, v_h) = 0 \qquad \forall v_h \in V_h^p, \tag{5}$$

where $L(u, u_h; \cdot,\cdot)$ is defined to be the bilinear form

$$L(u, u_h; e, v) = a(u, v) - a(u_h, v) = \int_0^1 a'[su + (1-s)u_h](e, v)ds, \tag{6}$$

where e denotes the error $e = u - u_h$, and $a'[w](\cdot, v)$ represents the functional derivative of the nonlinear form $a(\cdot, v)$.

To reduce over-shoots at shocks, we enhance (2) by shock–capturing terms

$$\sum_{K\in\mathbf{T}_h} c\,h^\alpha(|R(u_h)|\nabla u_h\cdot\nabla v_h)_K, \tag{7}$$

similar to the artificial viscosity model analyses by Jaffre *et al.* [6]; We note, that, due to the dependence on the cell residual $R(\cdot) = \nabla\cdot F(\cdot)$, the shock–capturing terms are consistent and hence do not violate the Galerkin orthogonality(4).

We discuss the question of *a posteriori* error estimation in terms of an arbitrary target functional $J(u)$ of the solution; typical examples include the outflow flux, local average and pointwise value, as well as the lift and drag coefficients of a body immersed in an inviscid fluid. By employing a duality argument and the Galerkin orthogonality (4), we derive the following *error representation* formula

$$J(u) - J(u_h) = \sum_{K \in \mathbf{T}_h} \{(R(u_h),\, z - z_h)_K + (r(u_h),\, z - z_h)_{\partial K}\}, \tag{8}$$

where $R(u_h)$ and $r(u_h)$ represent the cell and face residuals defined by

$$R(u_h)|_K = -\nabla \cdot F(u_h) \quad \text{and} \quad r(u_h)|_K = F(u_h) \cdot n - H(u_h, \hat{u}_h, n), \tag{9}$$

respectively, z_h stands for any discrete function $z_h \in V_h^p$, and z denotes the solution of the *dual problem*: find z such that

$$L(u, u_h; w, z) = J(w) \quad \forall w, \tag{10}$$

For simplification of notation, here the target functional $J(u)$ is assumed to be linear.
In order to render this error representation computable, we replace the (unknown) exact dual solution z in (8) by a numerical solution $\tilde{z}_h$ to following *approximate dual problem*, that is derived from (10) by linearization and discretization: find $\tilde{z}_h \in V_h^{\tilde{p}}$ such that

$$a'[u_h](w_h, \tilde{z}_h) = J(w_h) \quad \forall w_h \in V_h^{\tilde{p}}, \tag{11}$$

with $\tilde{p} > p$. This results in the following *approximate error representation*

$$J(u) - J(u_h) \approx \sum_{K \in \mathbf{T}_h} \eta_K, \tag{12}$$

where the cell terms

$$\eta_K = (R(u_h),\, \tilde{z}_h - z_h)_K + (r(u_h),\, \tilde{z}_h - z_h)_{\partial K}, \tag{13}$$

include the cell and face residuals multiplied by local weights involving the solution to the approximate dual problem (11).
Based on this *a posteriori* error estimate, and the so-called *weighted indicators* $|\eta_K|$, we design and implement the corresponding adaptive algorithm to ensure efficient and reliable control of the error in the computed functional. The performance of the proposed adaptive strategy is illustrated by a series of numerical experiments. In particular, we demonstrate the superiority of the proposed approach over standard mesh refinement algorithms which employ *ad hoc* error indicators.

References

[1] F. Bassi and S. Rebay. High-order accurate discontinuous finite element solution of the 2d Euler equations. *J. Comput. Phys.*, 138:251–285, 1997.

[2] R. Hartmann. Adaptive FE Methods for Conservation Equations. In H. Freistühler and G. Warnecke, editors, *Hyperbolic Problems: theory, numerics, applications: eighth international conference in Magdeburg, February, March 2000*, volume 2 of *International series of numerical mathematics; Vol. 141*, pages 495–503. Birkhäuser, Basel, 2001.

[3] R. Hartmann and P. Houston. Adaptive discontinuous Galerkin finite element methods for nonlinear hyperbolic conservation laws. Preprint 2001-20, (SFB 359), IWR Heidelberg, Mai 2001. submitted.

[4] R. Hartmann and P. Houston. Adaptive discontinuous Galerkin finite element methods for the compressible Euler equations. Preprint 2001-42, (SFB 359), IWR Heidelberg, Dez 2001. submitted.

[5] P. Houston, R. Rannacher, and E. Süli. A posteriori error analysis for stabilised finite element approximations of transport problems. *Comput. Meth. Appl. Mech. Engrg.*, 190(11-12):1483–1508, 2000.

[6] J. Jaffre, C. Johnson, and A. Szepessy. Convergence of the discontinuous Galerkin finite element method for hyperbolic conservation laws. *Math. Models and Methods in Appl. Sciences*, 5:367–386, 1995.

Using Richtmyer-Meshkov Driven Mixing Experiments to Impact the Development of Numerical Methods for Compressible Hydrodynamics

William J. Rider, James R. Kamm*, Cindy A. Zoldi, Katherine P. Prestridge, Christopher D. Tomkins, and Robert F. Benjamin

Los Alamos National Laboratory, Los Alamos, NM 87545, USA

Numerical methods for compressible hydrodynamics have improved dramatically during that past twenty years. One way to foster continued improvement of methods is to demand greater adherence to experimental observations. We describe a series of experiments that has provided a consistent challenge to computational algorithms. These involve shock-driven mixing initiated by the Richtmyer-Meshkov (RM) instability. An important aspect of these experiments is the spatial-temporal fidelity of the data. Recently, velocimetry data have been added to the repertoire. In addition, these experiments have been conducted on several different classes of initial conditions, leading to an extensive suite of calculations against which results can be validated.
Richtmyer-Meshkov experiments were conducted by Rightley et al. ([4]) at Los Alamos, and follow-on experiments have been conducted on the same apparatus. The experimental apparatus is a 5.5 m shock tube with a 75 mm^2 test section. The driver section is pressurized before the shot, and the rupturing of a polypropylene diaphragm produces a Mach 1.2 planar shock. In the test section, SF_6 gas is injected vertically through a nozzle in the top, and removed through an exhaust plenum at the bottom. Interchangeable nozzles with different contours impose perturbations on the cross section of the SF_6, which has a downward velocity of $\sim$ 10 cm/s. Earlier experiments used a sheet or "curtain" configuration with variations in the sheet thickness providing flow perturbations. Recent experiments have used single or double column(s) of SF_6. The evolving flow, which is imaged by a horizontal laser light sheet, is engineered so that the evolution remains approximately two-dimensional for the span of the experiment (although it eventually transitions to a fully three-dimensional flow). A tracer material consisting of glycol fog (with a typical droplet dimension of 0.5 μm) is added to the SF_6 to greatly enhance the dynamic range of the images, which are captured by CCD camera. There are additional experimental configurations that have been examined recently. A sample of these configurations is displayed in Figure 1. An additional camera has been added to implement a particle image velocimetry (PIV) capability. This system has produced high-resolution velocity fields for these experiments. We note that the integral scale Reynolds number for these flows is $\sim$20,000. If sufficient time is allowed for the flow to evolve one might expect a transition to a turbulent mixed state (a mixing transition [2]).
With the high-fidelity experimental data we can compare corresponding computations at a broad range of scales over a significant span of time. Fundamental to this process is the use of *quantitative* measures, by which experiment and calculation are compared ("code validation"); we also require that our comparisons improve under mesh refinement (i.e., that the calculations be "verified" [5]). One cannot expect to compare the simulations in a pointwise sense, due to the nature of the flow instabilities. Instead, we seek a spatial statistical congruence at corresponding times, where scale-dependent quantities are compared. To accomplish this, we use the following statistical techniques to characterize the data: correlations, fractals, and wavelets. We seek to make this comparison in as unbiased a manner as possible, where simulation data and experimental results are treated identically.
We have examined numerical solutions obtained with a spectrum of high-resolution numerical methods (TVD, second-order Godunov, WENO, PPM, and DG). Each of these "standard" methods produces the same basic behavior, which is retained under mesh refinement. These generic simulation characteristics are not consistent with the comparable experimentally observed scale-dependent behavior. As an example, we can look at our results with the usual limited Fromm scheme generalized to multidimensional interpolation [1]. As in our experience with other "standard" high-resolution methods, the results are neither qualitatively nor quantitatively like those seen in the experiments. This limiter can be modified in a manner so that it produces a modified equation with a Smagorinsky-like nonlinear viscosity. In this form, the velocity reconstruction is multiplied by the ratio of the velocity difference in a zone to its magnitude. When multiplied through a quadratic nonlinear, a Smagorinsky-like term is produced. We now examine the performance of this limiter when used to replace our standard monotone limiter in simulating the gas curtain, and computed using a modified version of the Cuervo code ([3]). Results are shown in Fig. (2) and statistically in Fig. (3). The statistical comparison of the standard high-resolution method is also shown in Fig. (3). These results suggest that with the adaptive time limiter are superior to those wih the standard methods, which exhibit characteristics that are fundamentally different from the experimental data.
We have begun the examination of numerical simulations on the cylinder configurations. For the single and the double cylinders, we replicate much of the experience with the curtain configuration, that is, the standard high-resolution methods have difficulty with the details of the flow. In these cases, however, this disagreement includes gross qualitative features exhibited in the experiments. This observation is quite obvious in the double cylinder configuration, where the experimental data show that, at

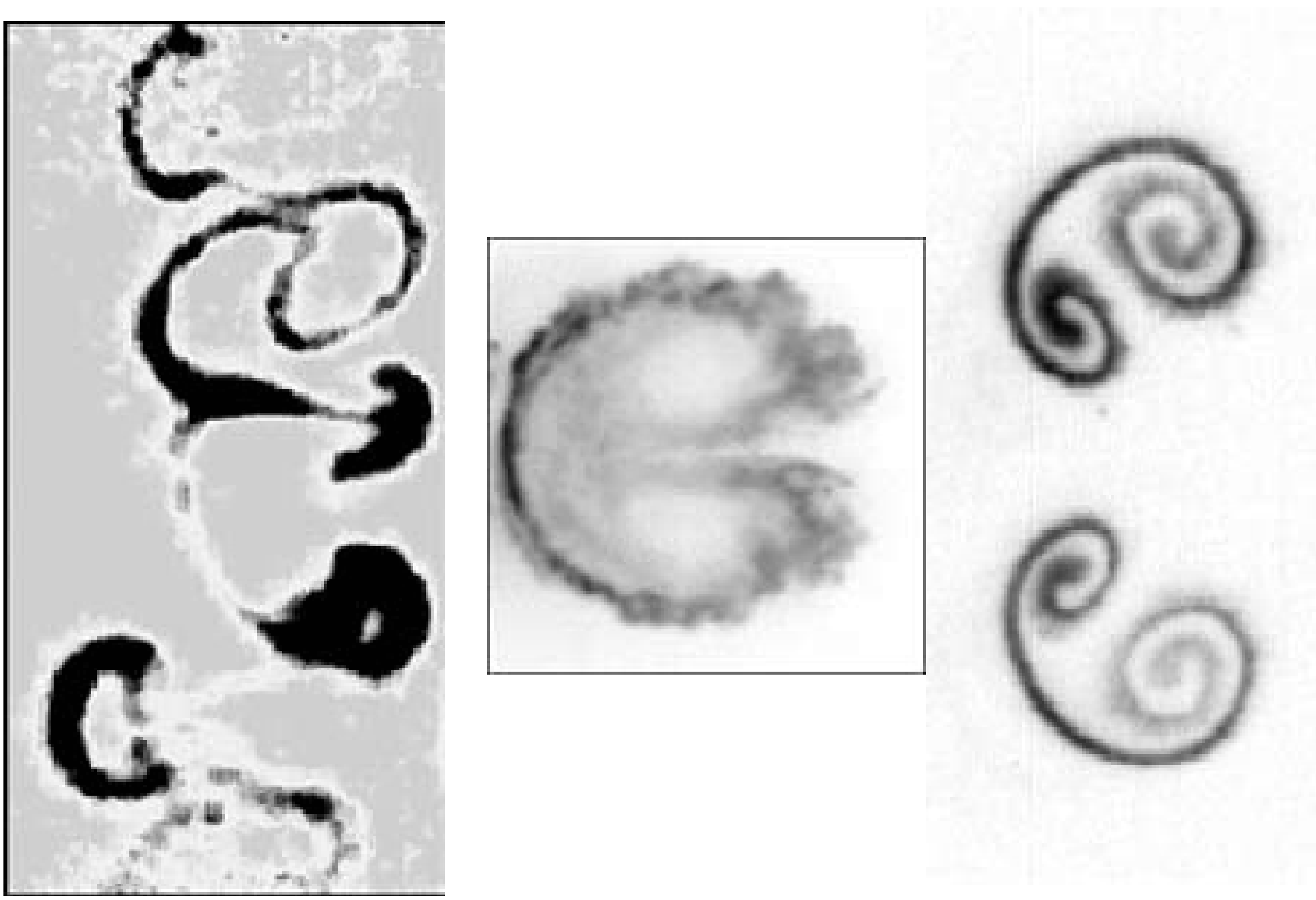

Figure 1: Here the three main experimental configuations are displayed. From left to right is the curtain (at 400 μs), the single cylinder (at 750 μs) and the double cylinder (at a separation of $2D$ and at 750 μs).

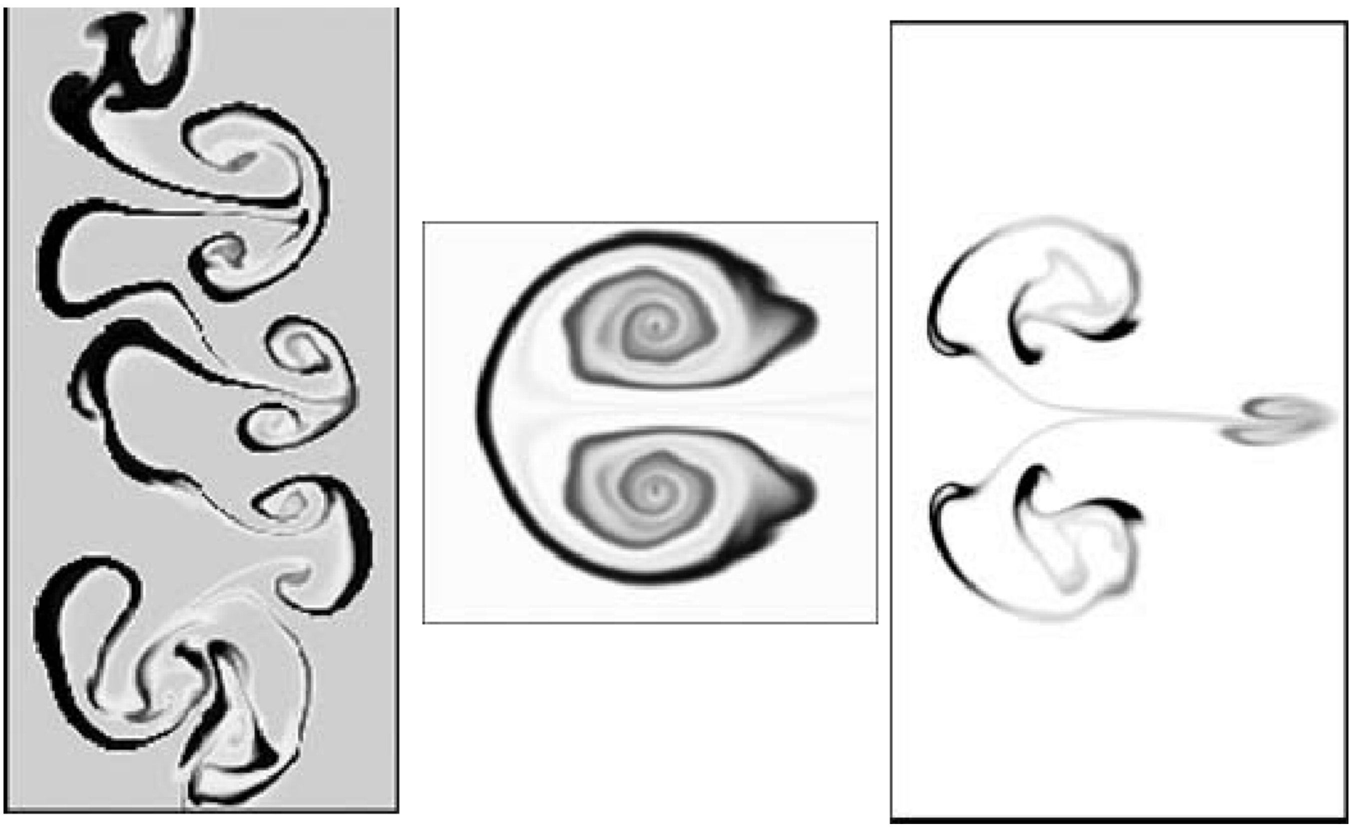

Figure 2: Here the three main experimental configuations as simulated by high resolution methods. From left to right is the curtain (at 400 μs), the single cylinder (at 750 μs) and the double cylinder (at an initial separation of $2D$ and at 750 μs). The gas curtain is initialized by the experimentally measured conditions, the others were initialized analytically.

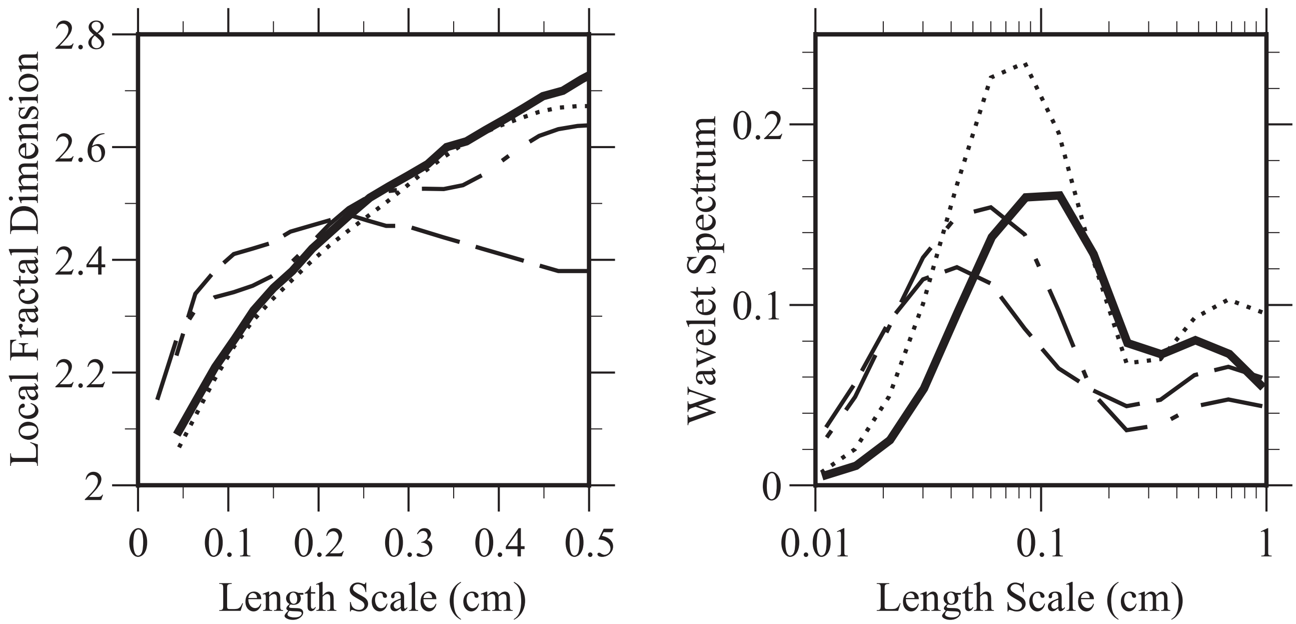

Figure 3: The comparison of the gas curtain simulations and experiments with statistical measures. The left shows the fractal dimension comparison while the right is the continuous wavelet spectrum analysis. The solid line shows the experiment, the long dashed method shows the high resolution method, the dotted line a first-order method and the dash-dot line is the adaptive time limiter. In general, the adpative time limiter solution is the most consistent with the experimental data.

a large initial separation, the SF_6 in the cylinders does not mix (see Figure 1), while the numerical calculations with standard methods show the formation of a jet between the cylinders (see Figure 2); moreover, this behavior is retained under mesh refinement. Intriguingly, the same modifications of the standard methods that improve the statistical congruence in the curtain configuration also remove the strong inter-cylinder jet from the double cylinder configuration.

In summary, we find under-resolved simulations of the Euler equations using several standard higher order methods to simulate these RM experiments compare poorly with the experimental data when quantified with these spatial statistics. The integral scale comparisons, however, remain acceptable and consistent with expectations for this class of methods. The most surprising result is that a first-order Godunov method produces a good comparison relative to the high-resolution methods. We find, however, that a simple modification that mimics turbulence modeling improves results significantly while retaining nominal second-order accuracy. The other approach that has shown great promise for improving the results is adaptive time differencing. Examining the solution near critical points where the time-derivative changes sign suggests that these points may lead to much of the discrepancy between the computed solutions and the experimental data. Using an adaptive time differencing separate from the adaptive spatial differencing greatly improves results.

These results are not meant to imply that high-order methods should not be used; rather, our viewpoint is that the high-order methods are not presently suitable for inviscid simulations of shock-induced compressible mixing if congruence in spatial statistics is desired. These methods need to be modified to improve results. We speculate that some aspects of high-resolution methods for multidimensional compressible flows may be undermining the statistical scaling in these Richtmyer-Meshkov simulations.

Lastly, we observe that experiments with high fidelity diagnostics were critical to uncovering these issues. At present, our numerical results for shock-driven mixing are far outside the experimental error and show qualitatively different details. Of course, we would be delighted to have flow diagnostics of even higher spatial resolution. We argue that quantitative "apples to apples" comparisons of experimental data with numerical results provide the most meaningful and compelling measure of the fidelity of numerical simulation. As we have mentioned, most commonly used methods produce less than satisfactory results, from which a number of unsettling conclusions can be drawn. A more pleasing conclusion would be to incite an effort to improve results via improving the algorithms. History suggests that carefully collected experimental observations have proven to be a driving force for improving theory in science. We contend that these experiments offer similar potential in the field of compressible hydrodynamics algorithms.

References

[1] T. J. Barth, ”Aspects of Unstructured Grids and Finite-Volume Solvers for Euler and Navier-Stokes Equations, VKI/NASA/AGARD Special Course on Unstructured Grid Methods for Advection Dominated Flows AGARD Publication R-787, 1995.

[2] P. Dimotakis, The mixing transition in turbulent flows, *J. Fluid Mech.*, **409**:69–98, 2001

[3] W. J. Rider, An Adaptive Riemann Solver Using a Two-Shock Approximation, *Comp. Fluids*, **28**:741–777.

[4] P. M. Rightley, P. Vorobieff, R. Martin & R. F. Benjamin, Experimental-observations of the mixing transition in a shock-accelerated gas curtain, *Phys. Fluids*, **11**:186–200, 1999.

[5] P. J. Roache, *Verification and Validation in Computational Science and Engineering*, Hermosa, Albuquerque, NM, 1998.

4.15 Tuesday, Session 2 (morning): Nonlinear waves

Nonlinear interactions of wavepackets in a periodic media

A. Babin

Department of Mathematics, University of California at Irvine, Irvine CA 92697-3875, U.S.A.

We develop a consistent mathematical theory of weakly nonlinear periodic dielectric media for the dimensions one, two and three. The theory is based on the Maxwell equations with quadratic and cubic constitutive relations. The relations include time delays. Solutions of the Maxwell equations on long time intervals are expanded in convergent series with respect to a small parameter α, which measures the contribution of the nonlinearity. After that we investigate in detail the principal term of the expansion in the case where the excitations (and, consequtively, solutions) have a form of wavepackets. The ratio ϱ of the amplitude frequency and the carrier frequency of a wavepacket is an important small parameter, $\varrho << 1$. The principal term describes the nonlinear interaction of different modes and is written in the form of an oscillatory integral. The phase function of the integral is written in terms of the Floquet-Bloch dispersion relations of the periodic media. This integral is of order ϱ^{q_0}, where q_0 is different for different combinations of interacting modes. We give a classification of the nonlinear interactions between wavepackets in a media with generic dispersion relations based on indices q_0. The indices q_0 take on only a relatively small number of prescribed values collected in a table, their values depend on a type of degeneracy of phase functions formed by the dispersion relations of the media. The crucial role in selecting the strongest interactions, in particular the second harmonic generation, is played by internal symmetries of the phase function.

Stability of Detonation Waves

Gregory Lyng

Indiana University, USA

We discuss recent results regarding the stability of strong detonation waves, particular traveling wave solutions of the equations of reacting flow. We describe how the Evans function framework for the stability analysis of shock waves, developed by R.A. Gardner and K. Zumbrun [GZ], can be applied to the more complicated setting of combustion. We discuss two results: (i) the evaluation of a *stability index*; and (ii) a stability result for small values of the heat release parameter, q.
An important feature of the work is the treatment of the *physical* system including gas dynamical and dissipative effects. Previous work has been restricted to the ZND model, in which dissipative effects are neglected, or the Majda model, in which the gas dynamical effects are modeled by a scalar conservation law.
The key tool of the analysis is the Evans function, $D(\lambda)$, an analogue to the characteristic polynomial. The quantity sgn $D'(0)D(+\infty)$ is the *stability index*; it provides a necessary condition for linear stability. We describe the evaluation of this stability index for strong detonation waves.
We also discuss a result for small q which extends a corresponding result by Liu and Ying [LYi] for the Majda model. Noting a reduction when $q = 0$, we obtain: *If the limiting viscous shock is stable, then so is the strong detonation for small q. In particular small amplitude strong detonations exist and are stable for small q.*

REFERENCES

[GZ] R. Gardner and K. Zumbrun, *The gap lemma and geometric criteria for the instability of viscous shocks*, Comm. Pure Appl. Math. 51 (1998), no. 7, 797-855.

[LYi] T. Liu and L. Ying, *Nonlinear stability of strong detonations for a viscous combustion model*, SIAM J. Math. Anal. 26 (1995), no. 3, 519-528.

Phase Transitions and Chapman-Jouguet Combustions

Andrea Corli

Department of Mathematics - University of Ferrara, Italy

We consider a system of conservation laws of the form

$$\partial_t u + \partial_x f(u) = 0 \,, \tag{1}$$

where $t \in [0,+\infty[$, $x \in \mathbf{R}$, $u \in \Omega$ with $\Omega \subseteq \mathbf{R}^n$ and the function $f\colon \Omega \mapsto \mathbf{R}^n$ is smooth. Ω is the disjoint union of two *phases* Ω_0, Ω_1. The system (1) is strictly hyperbolic in Ω with each characteristic field either genuinely nonlinear or linearly degenerate. For $i = 1,\ldots,n$, $\lambda_i(u)$ is the i-th eigenvalue of $Df(u)$. System (1) can be used to model non stationary phase transitions in a real fluid, with Ω_1 being the vapor phase and Ω_0 the liquid phase, as well as a chemical reaction such as a combustion. In the latter case, Ω_0 is the unburnt gas, while Ω_1 is the burnt gas.
Consider two states $\underline{u}^l \in \Omega_1$ and $\underline{u}^r \in \Omega_0$ belonging to different phases and assume that the Riemann problem with initial data $(\underline{u}^l, \underline{u}^r)$ has a solution $\underline{u}$ attaining only the values $\underline{u}^l$ and $\underline{u}^r$, separated by a jump propagating with speed $\underline{\Lambda}$. We define such a discontinuity *phase transition* and the line $x = \underline{\Lambda} \cdot t$ is the corresponding *phase boundary*.
In the present talk we overview some recent and new results related to the long time stability of the solution $\underline{u}$ with respect to $\mathbf{BV}$-small perturbations of the initial datum. This problem needs entirely different treatments and techniques depending on the the number of characteristics diverging from the unperturbed phase boundary $x = \underline{\Lambda} \cdot t$. If the number of characteristics diverging from the phase boundary is $n-1$, then the Riemann Problem for (1) is underdetermined for initial data close to $(\underline{u}^l, \underline{u}^r)$. This situation was studied in [2]. In the case of reacting gases, an example is provided by Chapman-Jouguet detonations. Under a suitable stability condition, there exists a unique solution to perturbed Riemann problems. This solution may well contain compound waves, i.e. rarefactions attached to a (sonic) phase boundary. It is of interest to note that the present underdeterminacy is solved introducing a constraint in the *structure* of the solution, without asking for any other admissibility condition.
Assume now that n characteristics diverge from the phase boundary. More precisely, let $\underline{\Lambda} = \lambda_k(\underline{u}^l) \in \,]\lambda_{k-1}(\underline{u}^r), \lambda_k(\underline{u}^r)[$, with k denoting a suitable genuinely nonlinear characteristic family. It is well known that a small perturbation of the initial data may lead either to a 1-underdetermined problem or to a 2-underdetermined. An example of this situation is given by Chapman-Jouguet deflagrations. Here, the Riemann problem is more severely underdetermined than in the previous case and a further admissibility condition needs to be imposed. Differently form the usual habits, we do not impose any condition motivated by physical *a priori* condition; rather, we introduce a fairly general condition and impose only those assumptions that lead, *a posteriori*, to a well-posed problem. More precisely, we require the presence of a smooth function $\Psi\colon (\Omega_1 \times \Omega_0) \cup (\Omega_0 \times \Omega_1) \mapsto \mathbf{R}$ so that the phase transition between u^l and u^r is said Ψ*-admissible* if, besides the usual Rankine-Hugoniot conditions, also $\Psi(u^l, u^r) = 0$ holds. This criterion generalizes both the *kinetic criterion* of [1] and the *visco-capillarity* criterion of [3]. The Riemann solver so introduced, inspired by combustion theory, provides unique solutions. Compound waves may well appear.
To obtain the well posedness of the Riemann problem we need both a compatibility condition and a stability assumption relating Ψ and f. The compatibility condition means, roughly speaking, that the function Ψ must be adapted to the sonic structure of the problem. The stability condition, on the other hand, generalizes Majda's condition for large shock waves.
The above results exploit the technique of wave front tracking and depend on interaction estimates suitably adapted to the speciufic structure of the problem. It is remarkable that several difficulties are entirely similar to those arising in the study of *nonconvex* systems of conservation laws.

References

[1] R. Abeyaratne and J. K. Knowles. Kinetic relations and the propagation of phase boundaries in solids. *Arch. Rational Mech. Anal.*, 114(2):119–154, 1991.

[2] R. M. Colombo and A. Corli. Sonic hyperbolic phase transitions and Chapman-Jouguet detonations. *J. Differential Equations*, to appear.

[3] M. Slemrod. Admissibility criteria for propagating phase boundaries in a van der Waals fluid. *Arch. Rational Mech. Anal.*, 81(4):301–315, 1983.

4.16 Tuesday, Session 2 (afternoon): Viscosity and shock waves

Effects of Viscosity on a Shock Wave Solution of the Euler Equations

Marco Kupiainen* and Gunilla Kreiss

NADA, KTH, Sweden

The Euler equations with an equation of state admitting multiple solutions to Riemann problems is considered. In Wendroff [1] several types of instabilities are investigated numerically using the Lax-Friedrichs scheme on a staggered grid. Here we re-examine one case, a Riemann problem where the end states can be connected with a 3-shock or with two shockwaves and an intermediate state. With discontinous initial data the Lax-Friedrichs scheme produces the solution with the intermediate state. Further computations show that with sufficiently smooth initial data the Lax-Friedrichs scheme produces the discrete 3-shock wave solution. Similar results are obtained with other schemes, however we note that the smoothness requirement (in order to obtain a 3-shock solution) of the initial profile is dependent on the numerical method used. To understand this behaviour we investigate the stability of a corresponding viscous problem. The viscosity is motivated by the numerical viscosity introduced to the solution by the Lax-Friedrichs scheme. Since reality is not invicid and the solution to this problem is sensitive to the smoothness of the initial profile one must consider if the Riemann problem with discontinous initial data is really relevant. If discontinous initial data is physically relevant, then one cannot conclude that the solution with the intermediate state is incorrect.

References

[1] Burton Wendroff: *A study of Non-uniqueness and Instability for Convex Materials*, Third International Conference on Hyperbolic Problems, Theory, Numerical Methods and Applications, pages 957-973, Studentlitteratur, 1990

Strong shocks of hyperbolic systems of conservation laws as viscous limits

Frédéric Rousset

UMPA, ENS Lyon, FRANCE

We consider a one dimensional system of conservation laws

$$u_t + f(u)_x = 0 \tag{1}$$

with a smooth flux $f : \mathbf{R}^n \to \mathbf{R}^n$. We assume that this system is strictly hyperbolic: $df(u)$ is diagonalizable with real simple eigenvalues. We denote by $\lambda_k(u)$ the eigenvalues and by $r_k(u)$ the right eigenvectors. We consider a solution u of (1) in the distributional sense which is piecewise smooth with a single shock, that is to say u is smooth at any point (x,t), such that $x \neq s(t)$ where $x = s(t)$ is a smooth curve, the limits

$$\partial_x^k u^-(t) = \lim_{x \to s(t)^-} \partial_x^k u(t,x),$$

$$\partial_x^k u^+(t) = \lim_{x \to s(t)^+} \partial_x^k u(t,x),$$

exist and $u^+(t)$ and $u^-(t)$ satisfy the Rankine-Hugoniot condition

$$f(u^+(t)) - f(u^-(t)) = s'(t)(u^+(t) - u^-(t)).$$

We also assume that the shock is a Lax p shock :

$$\lambda_1(u^-(t)) < \ldots < \lambda_{p-1}(u^-(t)) < s'(t) < \lambda_p(u^-(t)) < \ldots < \lambda_n(u^-(t)),$$
$$\lambda_1(u^+(t)) < \ldots < \lambda_p(u^+(t)) < s'(t) < \lambda_{p+1}(u^+(t)) < \ldots < \lambda_n(u^+(t)).$$

A general conjecture is that the admissible solutions of (1) should be obtained as limits of solutions of the viscous equation

$$u_t^\varepsilon + f(u^\varepsilon)_x = \varepsilon u_{xx}^\varepsilon. \tag{2}$$

Hence, we are interested in finding conditions on u so that u can be obtained as a viscous limit of (2).
Assuming that $\lambda_p(u)$ is genuinely nonlinear ($d\lambda_p \cdot r_p \neq 0$), Goodman and Xin [5] have shown that there exists a solution of (2) such that

$$u^\varepsilon \to u \qquad \text{in } L^\infty([0,T], L^2)$$

when $\varepsilon \to 0$ if

$$\sup_{t\in[0,T]} |u^+(t) - u^-(t)| \leq \eta \tag{3}$$

for some η sufficiently small.
In the proof of this result, the smallness assumption (3) is used twice. At first they use the fact that weak shocks admit viscous shock profiles that is to say solutions of

$$\begin{aligned} &\partial_{\xi\xi} V(\xi,t) = \partial_\xi\Big(f(V) - s'(t)V\Big) \\ &V(+\infty,t) = u^+(t), \\ &V(-\infty,t) = u^-(t). \end{aligned} \tag{4}$$

The existence of viscous shock profiles is shown by a center manifold technique. Next they build an approximate solution $u^{\,app}$ of (2) using technique of matched asymptotic expansions. More precisely, outside of the shock layer, they build an expansion

$$O(t,x) = u(t,x) + \varepsilon u^1(t,x) + \ldots$$

where u is the shock that we consider. Inside of the shock layer, they build an expansion

$$I(t,x) = V\left(\frac{x-s(t)}{\varepsilon} + \delta(t), t\right) + \varepsilon V^1\left(\frac{x-s(t)}{\varepsilon} + \delta(t), t\right) + \ldots$$

where $V(\cdot,t)$ is the viscous shock profile and $\delta(t)$ which is the perturbation of the shock position also has an expansion

$$\delta(t) = \delta_0(t) + \varepsilon\delta_1(t) + \ldots.$$

They then choose for u^ε the solution of (2) with initial data $u^{\,app}(0,\cdot)$. To show the convergence they have linearized (2) about u^{app} and integrated the equation obtained. Finally they prove the convergence by using energy estimates on the integrated equation

$$w_t + df(u^{app})w_x - \varepsilon w_{xx} = Q(w_x) + R^\varepsilon$$

where R^ε is small with respect to ε. Their weighted energy estimate is efficient only if the smallness assumption (3) is satisfied. This is linked with the linear stability of the viscous shock profiles. Weak shock profiles are linearly and nonlinearly stable [4]. Hence Goodman and Xin used that weak shocks which satisfy (3) admit viscous shock profiles which are linearly stable.
Among the various admissibility criteria of shocks for the hyperbolic system (1), one is the viscous profile criterion [2]: for t fixed, the shock $(u^-(t), u^+(t), s'(t))$ is admissible if it has a linearly stable viscous shock profile.
Our aim is to show that if for each $\tau \in [0,T]$ there exists a viscous profile $V(\xi,\tau)$ solution of (4) which is linearly stable, then there exists a solution u^ε of (2) which tends to u when ε tends to zero.
Let us formalize our hypothesis of linear stability: we consider the linear operator

$$L_\tau v = v'' - \Big(df(V(x,\tau) - s'(\tau)\Big)v'$$

with the limit conditions $v(+\infty) = 0$, $v(-\infty) = 0$. We say that a viscous profile is linearly stable if the solutions of

$$\partial_t v = L_\tau v,$$

$$v(0,x) = v_0(x)$$

tend to zero when t tends to $+\infty$. This is linked with the spectrum of the operator L_τ. The essential spectrum of $\mathcal{L}_\tau$ is confined in $\{\mathcal{R}e\,\lambda < 0\} \cup \{0\}$. In the right half-plane $\{\mathcal{R}e\,\lambda \geq 0\}\backslash\{0\}$ there are only eigenvalues. Using [3], [1], there exists an analytic function $D_\tau(\lambda)$ called the Evans function such that for $\mathcal{R}e\,\lambda \geq 0,\ \lambda \neq 0,\ \lambda$ is an eigenvalue of L_τ if and only if $D_\tau(\lambda) = 0$. The work of Zumbrun and Howard [8] shows that the linear stability of the viscous profile is characterized by the Evans function criterion

$$(\mathbf{H}_\tau) \qquad D_\tau(\lambda) \neq 0,\ \forall\lambda,\ \mathcal{R}e\,\lambda \geq 0.$$

Our theorem is

Theorem[7]

Assuming that u is a p Lax shock which has a smooth viscous profile $V(\xi,\tau)$ solution of (4) that satisfies ($\mathbf{H}_\tau$) for every $\tau \in [0,T]$, then there exists a solution u^ε of (2) such that

$$u^\varepsilon \to u \qquad \textit{in } L^\infty([0,T], L^1)$$

when ε tends to zero.

To prove the theorem , we first check that ($\mathbf{H}_\tau$) allows us to build high order inner and outer expansions I and O as in [5] without using the approximate diagonalization which is only efficient for weak shocks. It is the assumption $D_\tau(0) \neq 0$ that allows to do this construction.
To estimate $u^\varepsilon - u^{app}$, we follow the approach of [6], we build a Green's function $G(t,x,\tau,y)$ for the linear operator

$$L^\varepsilon w = w_t + df(u^{app})w_x - \varepsilon w_{xx}.$$

This means that the solution of

$$L^\varepsilon w = F,$$

$$w(0,x) = w_0(x)$$

can be written as

$$w(t,x) = \int G(t,x,0,y)w_0(y) + \int_0^t \int G(t,x,\tau,y)F(\tau,y)\,dyd\tau.$$

It is easy to show the convergence for the nonlinear problem if the Green's function satisfies the estimates

$$\sup_{\tau\in[0,T],y} \int |G^\varepsilon(t,x,\tau,y)|\,dxdt \leq C, \tag{5}$$

$$\sup_{\tau\in[0,T],y} \int |\partial_x G^\varepsilon(t,x,\tau,y)|\,dxdt \leq \frac{C}{\sqrt{\varepsilon}}, \tag{6}$$

where C depends on T but is independent of ε. To build the Green's function G^ε, we use the iterative construction of Green's functions of [6] which relies on the choice of various approximate Green's functions. In particular, we use the Green's function of the operator that is obtained by freezing the time in the shock layer. For this Green's function, very precise estimates are known [8].

References

[1] S. Benzoni-Gavage, D. Serre, and K. Zumbrun. Alternate Evans function and viscous shock waves. *SIAM J. Math. Anal*, 32:929–962, 2001.

[2] C. M. Dafermos. *Hyperbolic conservation laws in continuum physics*. Springer-Verlag, Berlin, 2000.

[3] R. A. Gardner and K. Zumbrun. The gap lemma and geometric criteria for instability of viscous shock profiles. *Comm. Pure Appl. Math.*, 51(7):797–855, 1998.

[4] J. Goodman. Nonlinear asymptotic stability of viscous shock profiles for conservation laws. *Arch. Rational Mech. Anal.*, 95(4):325–344, 1986.

[5] J. Goodman and Z. P. Xin. Viscous limits for piecewise smooth solutions to systems of conservation laws. *Arch. Rational Mech. Anal.*, 121(3):235–265, 1992.

[6] E. Grenier and F. Rousset. Stability of one-dimensional boundary layers by using Green's functions. *Comm. Pure Appl. Math.*, 54(11):1343–1385, 2001.

[7] Rousset (F.). – Viscous limits for strong shocks of systems of conservation laws. *Preprint*, 2001.

[8] K. Zumbrun and P. Howard. Pointwise semigroup methods and stability of viscous shock waves. *Indiana Univ. Math. J.*, 47(3):741–871, 1998.

Numerical approximation of the Navier-Stokes equations with several independent specific entropies

C. Chalons*

ONERA and École Polytechnique, Paris

F. Coquel

CNRS and Université Paris VI, Paris

The present work is devoted to the numerical approximation of the solutions of convective-diffusive systems which will be understood as natural extensions of the classical Navier-Stokes (NS) equations. Solutions of these systems are governed by N ($N \geq 2$) independent pressure laws or equivalently N independent specific entropies. Several models from the physics actually enter the present framework. These extended forms of the usual NS equations (e.g. when $N = 1$) will be seen to share many properties but with the very difference that, generally speaking, they cannot be recast in full conservation form. This property is known to make the definition of the endpoints of the Travelling Wave (TW) solutions sensitive with respect to the shape of the diffusive tensor. Here, we exhibit $(N-1)$ Generalized Rankine-Hugoniot (GRH) conditions that reflect this sensitivity. We underline the reason why classical algorithms can only fail in satisfying these GRH relations and we show how to enforce them for validity at the discrete level. Several numerical evidences are proposed.

The mathematical model and some basic properties

In this work, we are interested in the numerical approximation of the solutions of the following convective-diffusive system (in one space dimension for simplicity) :

$$\begin{cases} \partial_t \rho + \partial_x \rho u = 0, \qquad x \in I\!R, \quad t > 0, \\ \partial_t \rho u + \partial_x (\rho u^2 + \sum_{i=1}^N p_i) = \partial_x ((\sum_{i=1}^N \mu_i) \partial_x u), \\ \partial_t \rho \epsilon_i + \partial_x (\rho \epsilon_i u) + p_i \partial_x u = \mu_i (\partial_x u)^2, \quad i = 1, ..., N, \end{cases} \tag{1}$$

where with classical notations, $\rho, \rho u$ and $\{\rho\epsilon_i\}_{i=1,\dots,N}$ respectively denote the density, the momentum and N independant internal energies. Before addressing the required closure relations, let us stress that (1) is nothing but a natural extension of the usual NS equations : namely when considering a single pressure law. Here, N ($N \geq 2$) independent pressure laws $p_i(\rho, \rho\epsilon_i)$ are involved via N independent governing equations for each of the $\rho\epsilon_i$. In (1) and for $i = 1, \dots, N$, μ_i ($\mu_i \geq 0$) denotes a smooth mapping standing for the viscosity law associated with the internal energy $\rho\epsilon_i$. It will be always assumed that $\mu := \sum_{i=1}^N \mu_i > 0$. Depending on the choice of the closure equation for defining each of the μ_i, several models from the physics enter the present framework. Let us quote for instance compressible turbulence models like the $k - \epsilon$ model (see Berthon-Coquel [1]), and more generally multi-scale models (see Chalons [2] and [3]) or models coming from the plasma physics (see Cordier et al. [5], Coquel-Marmignon [4]).

Now considering the required closure equations for defining each of the N pressure laws, we shall assume that according to the second principle of the thermodynamics :

$$-T_i(\tau, \epsilon_i) ds_i = d\epsilon_i + p_i(\tau, \epsilon_i) d\tau, \quad \tau = 1/\rho, \tag{2}$$

defines a strictly convex smooth mapping $(\tau,\epsilon_i) \to s_i(\tau,\epsilon_i)$ for any given $i \in \{1,..,N\}$. In addition, each pressure law is assumed to obey the well-known Weyl's assumptions (see [8] for the details). Notice that all the above assumptions are quite classical within the frame of the usual NS equations (e.g. with $N=1$). Owing to these assumptions, our first statement highlights the relationships with the usual setting, when defining the following natural phase space for (1):

$$\Omega = \{\mathbf{v} := (\rho, \rho u, \{\rho\epsilon_i\}_{1\le i\le N}) \in I\!R^{N+2}/\rho > 0,\ \rho u \in I\!R,\ \rho\epsilon_i > 0, \quad 1 \le i \le N\}. \tag{3}$$

Lemma *The first order extracted system from (1) is hyperbolic over Ω, with the following increasingly ordered eigenvalues :*

$$\lambda_1(\mathbf{v}) = u - c \le \lambda_2(\mathbf{v}) = \cdots = \lambda_{N+1}(\mathbf{v}) = u, \le \lambda_{N+2}(\mathbf{v}) = u + c,\ c^2(\mathbf{v}) = \sum_{i=1}^{N} c_i^2(\mathbf{v}),$$

where each partial sound speed is such that $c_i^2(\mathbf{v}) := (\partial_\rho p_i)_{s_i} > 0$. The $1-$ and $(N+2)-$ fields are genuinely nonlinear, all the other fields being (necessarily) linearly degenerate.
The system (1) naturally writes in non conservation form. This rises the question of the existence of an admissible change of variables that recasts (1) in full conservation form. With this respect, the next claim gives all the additional non trivial equations for the smooth solutions of (1) :
Theorem *Smooth solutions of (1) obey the following conservation law :*

$$\partial_t \rho E + \partial_x(\rho E + \sum_{i=1}^{N} p_i)u = \partial_x((\sum_{i=1}^{N}\mu_i)u\partial_x u), \tag{4}$$

where the total energy reads $\rho E = (\rho u)^2/2\rho + \sum_{i=1}^{N}\rho\epsilon_i$.. In addition, such solutions satisfy :

$$\partial_t \rho s_i + \partial_x \rho s_i u = -\frac{\mu_i}{T_i}(\partial_x u)^2, \quad i = 1, ..., N. \tag{5}$$

Up to classical nonlinear transformations in the $s_{i1\le i\le N}$, these are the only additional non trivial equations (without special assumptions on the $\{\mu_i\}_{1\le i\le N}$).
Let us rephrase the above result when investigating suitable change of variables for (1). Obviously, the three variables ρ, ρu and ρE are natural candidates since they are governed by conservation laws. Next and for completeness, let us consider without restriction the set $\{\rho s_i\}_{1\le i\le N-1}$ to define $\mathbf{u} := (\rho, \rho u, \rho E, \{\rho s_i\}_{1\le i\le N-1})$ as an admissible unknown. Then, smooth solutions of (1) equivalently satisfy :

$$\begin{cases} \partial_t\rho + \partial_x \rho u = 0, \qquad x \in I\!R, \quad t > 0, \\ \partial_t \rho u + \partial_x(\rho u^2 + \sum_{i=1}^{N} p_i) = \partial_x((\sum_{i=1}^{N}\mu_i)\partial_x u), \\ \partial_t \rho E + \partial_x(\rho E + \sum_{i=1}^{N} p_i)u = \partial_x((\sum_{i=1}^{N}\mu_i)u\partial_x u), \\ \partial_t \rho s_i + \partial_x \rho s_i u = -\frac{\mu_i}{T_i}(\partial_x u)^2, \quad i = 1, ..., N-1. \end{cases} \tag{6}$$

Now, let us emphasize that whitout further condition, smooth solutions of (6) automatically obey **with equality** the additional PDE :

$$\partial_t \rho s_N(\mathbf{u}) + \partial_x \rho s_N(\mathbf{u}) u = -\frac{\mu_N}{T_N}(\partial_x u)^2. \tag{7}$$

Hence, the pair $(\rho s_N, \rho s_N u)$ is nothing but a Lax entropy pair but with a **prescribed** rate of entropy dissipation. To go further in that direction, let us observe that despite the identities (5) might be understood as N fully independent equations, these do actually evolve **proportionally** according to :
Corollary *Smooth solutions of (6) obey :*

$$\mu_N T_i\{\partial_t \rho s_i + \partial_x \rho s_i u\} = \mu_i T_N\{\partial_t \rho s_N(\mathbf{u}) + \partial_x \rho s_N(\mathbf{u}) u\}, \quad i = 1, ..., N-1. \tag{8}$$

(8) expresses nothing but a trivial cancellation property in $(\partial_x u)^2$. However, this observation turns out to be crucial for our numerical purposes. Indeed when applied to TW solutions of (6), the identities (8) can be understood as $(N-1)$ Generalized Rankine-Hugoniot (GRH) conditions (see [3]).
Remark To exemplify the previous claim, let us temporarily adopt the following closure for the viscosity laws : $\mu_i(\mathbf{u}) = \mu_i^0 T_i$

where for each $i = 1, \dots, N$, μ_i^0 denotes a positive real number. Let us recall that such a closure can be inferred from the classical transport theory for dilute gases. Then, (8) are easily seen to boil down to :

$$\{\partial_t \rho(\frac{\mu_N}{\mu} s_i - \frac{\mu_i}{\mu} s_N(\mathbf{u})) + \partial_x \rho(\frac{\mu_N}{\mu} s_i - \frac{\mu_i}{\mu} s_N(\mathbf{u}))u\} = 0, \quad i = 1, ..., N-1. \tag{9}$$

Therefore, (9) clearly provide us with $(N-1)$ jump conditions that in addition to the three classical Rankine-Hugoniot conditions respectively for ρ, ρu and ρE, yield a complete set of jump relations for defining the endpoints of a TW solution of (6). Let us underline that such endpoints are clearly dictated by the ratios of the viscosities.
More generally, the proportionality in the evolution in time of all the entropy balance equations (as put forward in (8)) expresses a well-known property of general convective-diffusive systems in non conservation form. Namely, the endpoints of their TW solutions entirely depend on the shape of the diffusive tensor under consideration (see Dal Maso et al. [6] and LeFloch [7]). As underlined in the next section, this key property will make the numerical approximation of the TW solutions of (8) a challenging issue (see also [7]). In the present work, we show how to enforce numerically for validity the GRH relations (8), taking advantage of the following result :
Theorem *Smooth solutions of system (6) obey equivalently the following system in non conservation form :*

$$\begin{cases} \partial_t \rho + \partial_x \rho u = 0, \qquad x \in I\!R, \quad t > 0, \\ \partial_t \rho u + \partial_x(\rho u^2 + \sum_{i=1}^N p_i) = \partial_x((\sum_{i=1}^N \mu_i)\partial_x u), \\ \partial_t \rho E + \partial_x(\rho E + \sum_{i=1}^N p_i)u = \partial_x((\sum_{i=1}^N \mu_i) u \partial_x u), \\ \mu_N T_i\{\partial_t \rho s_i + \partial_x \rho s_i u\} - \mu_i T_N\{\partial_t \rho s_N(\mathbf{u}) + \partial_x \rho s_N(\mathbf{u}) u\} = 0, \ 1 \le i \le N-1. \end{cases} \tag{10}$$

Numerical approximation
In this section, we present a suitable numerical method for approximating the solutions of (10). We emphasize that several distinct methods have been actually developed and analysed in Chalons-Coquel [3] (see also [2]) to that purpose. Their design principle is always focused at preserving the validity of the GRH conditions we have put forward in (8). In addition, they all satisfy the same stability estimates but they come with a different cost of numerical evaluation. Here, we shall restrict ourselves to the most natural one (e.g. along the lines of the first section) but at the expense of the largest numerical cost. This method can be understood as a prediction-correction strategy. In the prediction step, we just propose to solve the equivalent form (6) with appropriate initial data. Such an approach sounds quite natural but however will be seen to fail in preserving the validity of the GRH conditions at the discrete level. Highlighting the roots of such a failure will naturally motivate the correction step which precisely aims at restoring the validity of (8) at each time step.
To avoid unnecessary cumbersome notations in this abstract, we shall only roughly describe these two steps. All the claims put forward below are rigourously proved in [2]. Let be given an approximate solution of the system (10), say $\mathbf{u}^h(x, t^n)$, at the time level t^n, where h stands for a space discretisation parameter. In order to advance this solution to the next time level $t^{n+1} := t^n + \delta t$, we propose two steps.
Prediction step. This step simply consists in solving for small times the Cauchy problem for (6) when considering $\mathbf{u}^h(x, t^n)$ as initial data. We classically approximate the solution performing a splitting between the convective and the diffusive parts. As far the second order operator is concerned :

$$\begin{cases} \partial_t \rho = 0, \\ \partial_t \rho u = \partial_x((\sum_{i=1}^N \mu_i)\partial_x u), \\ \partial_t \rho E = \partial_x((\sum_{i=1}^N \mu_i) u \partial_x u), \\ \partial_t \rho s_i = -\frac{\mu_i}{T_i}(\partial_x u)^2, \quad i = 1, ..., N-1, \end{cases} \tag{11}$$

we just have to solve $\rho^h(x, t^n)\partial_t u = \partial_x((\sum_{i=1}^N \mu_i)\partial_x u)$ with $u^h(x, t^n)$ as initial data and then update ρE and the $\{\rho s_i\}_{1 \le i \le N-1}$ accordingly. Several appropriate numerical techniques are at hand to provide an updated solution, namely $\mathbf{u}^h(x, t^{n+1=})$, which satisfies loosely speaking :

$$\frac{\rho s_n(\mathbf{u}^h(x, t^{n+1=})) - \rho s_n(\mathbf{u}^h(x, t^n))}{\delta t} = -\frac{\mu_N}{T_N}(\partial_x u)^2 \tag{12}$$

Such an identity just claims that the right hand side can be given a consistent definition in the sense of finite differences. Next turning considering the first order operator, we have to approximate the solution of the following Cauchy problem with initial

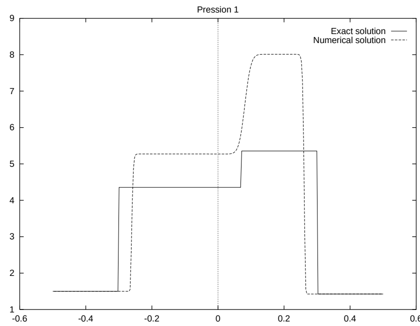

Figure 1: Numerical solution and exact one

data $\mathbf{u}^h(x, t^{n+1=})$:

$$\begin{cases} \partial_t \rho + \partial_x \rho u = 0, \\ \partial_t \rho u + \partial_x (\rho u^2 + \sum_{i=1}^N p_i) = 0, \\ \partial_t \rho E + \partial_x (\rho E + \sum_{i=1}^N p_i) u = 0, \\ \partial_t \rho s_i + \partial_x \rho s_i u = 0, \quad i = 1, ..., N-1, \end{cases} \tag{13}$$

supplemented with the following Lax entropy inequality :

$$\partial_t \rho s_N(\mathbf{u}) + \partial_x \rho s_N(\mathbf{u}) u \leq 0. \tag{14}$$

Let us underline that (14) is indeed needed for uniqueness of weak solutions of (13). Adopting for instance the Godunov method, we end up with an updated approximate solution $\mathbf{u}^h(x, t^{n+1-})$ but which satisfies (in a sense to be specified) :

$$\frac{\rho s_n(\mathbf{u}^h(x, t^{n+1-})) - \rho s_n(\mathbf{u}^h(x, t^n))}{\delta t} + \partial_x \rho s_n(\mathbf{u}^h(x, t^{n+1=})) u = -\frac{\mu_N}{T_N} (\partial_x u)^2 + \mathit{Error}.$$

Here, the *Error* term is classically made of the contribution of entropy satisfying shocks plus the contribution of the Jensen inequality (see [8] or [2] for the details). This *Error* is well-known to stay always non-positive. As a direct consequence, the cancellation property, responsible of (8), is lost and the GRH conditions can no longer be satisfied. Obviously, such a failure persists using a suitable Approximate Riemann solver for (13)–(14). Figure 1 displays a typical example, illustrating that approximate solutions grossly disagree with the exact one.

The above discussion clearly motivates the need for the following correction step to define the required updated solution $\mathbf{u}^h(x, t^{n+1})$.

Correction step. We keep unchanged the updated conservative variables, e.g. : $\rho^h(x, t^{n+1}) = \rho^h(x, t^{n+1-})$, $(\rho u)^h(x, t^{n+1}) = (\rho u)^h(x, t^{n+1-})$, $(\rho E)^h(x, t^{n+1}) = (\rho E)^h(x, t^{n+1-})$, and we propose to redefine the N specific entropies $s_i^h(x, t^{n+1})$ as the solutions of the following nonlinear algebraic problem :

$$\begin{array}{l} (\mu_N T_i)(x, t^{n+1-}) \left\{ \frac{\rho s_i(x, t^{n+1}) - \rho s_i(x, t^n)}{\delta t} + \partial_x \rho s_i(x, t^{n+1=}) u \right\} = \\ (\mu_i T_N)(x, t^{n+1-}) \left\{ \frac{\rho s_n(\mathbf{u}^h(x, t^{n+1})) - \rho s_n(\mathbf{u}^h(x, t^n))}{\delta t} + \partial_x \rho s_n(\mathbf{u}^h(x, t^{n+1=})) u \right\}, \end{array} \tag{15}$$

for $i = 1, \ldots, N$. Notice that (15) is nothing but a discrete version of the GRH conditions (8), this discrete version being directly inherited from the prediction step. It can be shown that solving (15) in fact amounts to solve a single nonlinear equation. The latter can be proved to admit an unique well-defined solution provided that the Approximate Riemann solver for (13) is entropy satisfying with respect to (14). In addition, positivity preserving properties as well as maximum principles for all the specific entropies can be proved to be preserved at the correction step. We refer the reader to [2] for the details. The next figure 2 strongly indicates that the proposed correction strategy fairly succeeds in producing approximate solutions in good agreement with the exact one. We refer the reader to [2], [3], for other suitable numerical methods again based on a prediction-correction strategy but for which, the correction step is fully explicit.

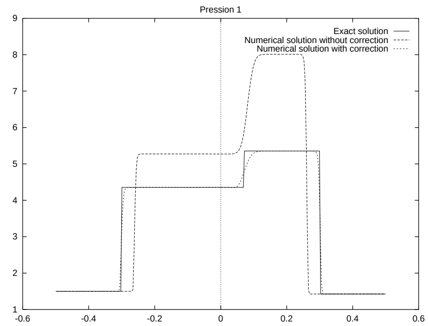

Figure 2: Numerical solutions and exact one

References

[1] C. BERTHON, F. COQUEL, *Nonlinear projection scheme to solve systems in non conservation form*, in Innovative methods in Computational Fluid Dynamics.

[2] C. CHALONS *Thesis*, in preparation.

[3] C. CHALONS AND F. COQUEL, works in preparation.

[4] F. COQUEL AND C. MARMIGNON, *A Roe-type Linearization for the Euler Equations for Weakly Ionized Gases* in Finite Volumes for Complex Applications II, Hermes (1999).

[5] S. CORDIER ET AL., Asymptotic Analysis, 10 (1995).

[6] G. DAL MASO, P. LEFLOCH, F. MURAT, *Definition and weak stability of a non conservative product*, in J. Math. Pures et Appli., vol 74 (1995).

[7] P.G. LEFLOCH *An introduction to Nonclassical Shocks*, in Lecture Notes in Computational Science and Engineering, 5 (1998).

[8] E. GODLEWSKI AND P.A. RAVIART Numerical Approximation of Hyperbolic Systems of Conservation Laws, Springer (1996).

Spectral energy methods and the stability of shock waves

Jeffrey Humpherys* and Kevin Zumbrun

Indiana University, USA

We will review and motivate the stability problem for viscous shock waves and discuss our recent work in proving strong spectral stability of small-amplitude shock profiles for physically realistic models, including gas dynamics and magnetohydrodynamics. Specifically, we use energy methods, extending the works of Goodman, Kawashima, Matsumura, Nishihara, etc., to prove one-dimensional spectral stability of small amplitude shock profiles for degenerate viscosity conservation laws that are dissipative symmetric-hyperbolic in the sense of Kawashima, generalizing the well-known results of Goodman and of Kawashima, Matsumura, and Nishihara. One distinction, however, is that our analysis is carried out in the frequency domain, rather than the space-time domain. It has been recently shown, for rather general systems of these types, that spectral stability implies nonlinear stability. Thus, the stability problem for viscous shocks is reduced to determining the character of the spectrum of the linearized evolution operator, whereby spectral stability is the key.

4.17 Tuesday, Session 3 (morning): Quantum hydrodynamics

Nonrelativistic Limit from Klein-Gordon Maxwell to Schrödinger Poisson

Norbert Mauser* and Sigmund Selberg

Wolfgang Pauli Inst. c/o Inst. f. Math., Univ Wien, Strudlhofg. 4, A–1090 Wien, Austria

We prove that in the nonrelativistic limit $c \to \infty$, where c is the speed of light, solutions of the time dependent Klein-Gordon-Maxwell system in 3 space dimensions converge in the energy space $C([0,T]; H^1)$ to solutions of a Schrödinger-Poisson system, under appropriate conditions on the initial data. This requires the splitting of the scalar Klein-Gordon field into a sum of two fields, corresponding, in the physical interpretation, to electrons and positrons. The crucial technique is to turn the Klainerman-Machedon machinery for the appropriatly scaled system which has null form structure in the case of Coulomb gauge.

The Limit from the Schrödinger-Poisson to the Vlasov-Poisson Equations with General Data in One Dimension

Ping Zhang

The Chinese Academy of Sciences, Beijing

Yuxi Zheng*

Indiana University

Norbert J. Mauser

University of Vienna

We will talk about the classical limit of the Schrödinger-Poisson system to the Vlasov-Poisson equations as the Planck constant ϵ goes to zero. This limit is also frequently called "semiclassical limit". The coupled Schrödinger-Poisson system for the wave functions $\{\psi_j^\epsilon(t,x)\}$ are transformed to the Wigner-Poisson equations for a "phase space function" $f^\epsilon(t,x,\xi)$. For the case of the so called "completely mixed state", i.e. $j = 1, 2, \cdots, \infty$, under additional assumptions on the potential, this classical limit has been solved in 1993 by Lions and Paul (Sur les measures de Wigner, *Rev. Mat. Iberoamericana*, **9**(1993)) and, independently, by Markowich and Mauser (*Math. Meth. Mod. Appl. Sci.*, **3**(1993)) with strong assumptions on the initial data. The so called "pure state" case where only one or a finite number of wave functions $\{\psi_j^\epsilon(t,x)\}$ are considered, has been open up to now.
We prove here for general initial data (pure state as well as mixed state case) of the wave functions in one space dimension that the Wigner measure $f(t,x,\xi)$, which is a weak limit of $f^\epsilon(t,x,\xi)$ as ϵ tends to 0, satisfies the classical 1-d Vlasov-Poisson equations. As a crucial prerequisite, we have improved the decay assumption on the initial data of 1-d Vlasov-Poisson equations in work by Yuxi Zheng and A. Majda, *Comm. Pure Appl. Math.*, **47**(1994) for the existence of global weak solutions with measures as initial data.
The equations we regard are widely used in quantum/classical transport and semiconductor theory as a nonlinear one particle ("mean field") approximation of the linear N electron Schrödinger/Hamilton equation.

Multi-Phase Computation of the Schrödinger Equation Multi-phase Computations of the SemiClassical Limit of the Schrödinger Equation

Shi Jin and Xiantao Li*

Department of Mathematics, University of Wisconsin-Madison, WI 53706, USA

We present and compare two different techniques to obtain the multi-phase solutions for the schrödinger equation in the semi-classical limit. The first is Whitham's averaging method, which gives the modulation equations governing the evolution of multi-phase equations. The second is the Wigner transform, a convenient tool to derive the semiclassical limit equation–the Vlasov equation–for the linear Schrödinger equation. Motivated by the linear superposition principle, we derive the multi-phase ansatz for the Wigner function by the stationary phase method, and then use the ansatz to close the Vlasov equations to obtain the multi-phase equations. We show that the multi-phase equations so derived agree with those derived by Whitham's averaging method. Generic way of obtaining and computing the multi-phase equations by the Wigner function is given, and kinetic schemes are introduced to solve these multi-phase equations. Several numerical examples are given to demonstrate the validity of this approach. Similar studies are conducted for the linearized Korteweg-de Vries equation and the linear wave equation.

4.18 Tuesday, Session 3 (afternoon): Central schemes I

Central Runge-Kutta Schemes for Conservation Laws

L. Pareschi

Università di Ferrara, Italy

G. Puppo*

Politecnico di Torino, Italy

G. Russo

Università di Catania, Italy

In this work we propose a new formulation for central schemes based on staggered cell averages for the integration of hyperbolic systems of conservation laws. The Central Runge Kutta (CRK) schemes we propose enjoy the simplicity of central schemes and their results are comparable with those given by older central schemes. However for schemes of order higher than 2, CRK schemes require less function evaluations, and are therefore more efficient.
These schemes have a predictor-corrector structure. Our preliminary numerical results show that it is necessary to use non linear weights in the reconstruction only in the corrector step. The predictor steps can be computed with a linear scheme.
In this work, we briefly outline the construction of CRK schemes, and we show numerical results on several test problems.

New semi-discrete central schemes for hyperbolic conservation laws

Chi-Tien Lin

Department of Applied Mathematics, Providence University, Shalu 43301, Taiwan

The main feature of central schemes is that they are Riemann-solver free. The original high-order central scheme by Nessyahu and Tadmor [NeTa] assumes a global speed of wave propagation which introduces a large amount of numerical viscosity and lows the resolution of discontinuities. Recently, Kurganov and Tadmor [KurTa] proposed a new version of central schemes In their construction, each control volume is divided into smooth and singular rectangular parts according to local speed of wave propagation. The update value at each gridpoints is obtained from more precise computation on each region resulting in sharper resolution and lower numerical viscosity. Their scheme can be formulated in a semi-discrete form and can be applied to solve conservation laws and convection-diffusion equations as well.

In Kurganov and Tadmor's construction, singular regions are secured in a sub-rectangular region. In this talk, we shall construct new semi-discrete central scheme by replacing the sub-rectangular singular region with a smaller triangular region in each controlled volume. We shall show lower numerical viscosity as excepted. Numerical simulation will be present to show sharper results.

References

[KurTa] Kurganov and Tadmor, *New High-Resolution Central Schemes for Nonlinear Conservation Laws and Convection-Diffusion Equations*, J. Comp. Physics,**160**, 200, 241-282.

[NeTa] H. Nessyahu and E. Tadmor, *Non-oscillatory Central Differencing for Hyperbolic Conservation Laws*, JCP, **87**, 1990, 408-463.

Central-Upwind Schemes for the Saint-Venant System

Alexander Kurganov

Tulane University, USA

Doron Levy*

Stanford University, USA

The Saint-Venant system is commonly used to model flows in rivers or coastal areas. This system describes the flow as a conservation law with an additional source term. In two space dimensions it takes the form

$$\begin{cases} h_t + (hu)_x + (hv)_y = 0, \\ (hu)_t + \left(hu^2 + \dfrac{1}{2}gh^2\right)_x + (huv)_y = -ghB_x, \\ (hv)_t + (huv)_x + \left(hv^2 + \dfrac{1}{2}gh^2\right)_x = -ghB_y, \end{cases} \tag{1}$$

where $B(x,y)$ represents the bottom elevation, h is the fluid depth above the bottom, (u,v) denotes the velocity field, and g is the gravitational constant. Several cases are of special interest for equation (1):

1. **The quasi-stationary state.** In the stationary state there is no motion, $u=0$, and the top surface is flat, $h(x,y,t)+B(x,y)=C$, for some constant C. A quasi-stationary state is generated by slightly perturbing the height of the stationary state. For example, in the one-dimensional case, assume a bottom topography in the shape of a hump, and a perturbation of the form $h = C - B(x) + \varepsilon(x)$, where ε is a compactly supported constant perturbation. In this case, the disturbance splits into two waves which, for small ε are essentially linear propagating at the characteristic speeds $\pm\sqrt{gh}$.

2. **A quasi-steady flow.** There are steady-states in which the momentum hu, is a nonzero constant. The different regimes of such a flow depend on the bottom topography and on the free-stream Froude number $\mathrm{Fr} = u/\sqrt{gh}$. If $\mathrm{Fr}<1$ or $\mathrm{Fr}>1$ everywhere, then the solution is smooth. For intermediate freestream Froude numbers the flow can be transcritical with transitions where Fr passes through 1, and hence one of the eigenvalues, $u\pm\sqrt{gh}$ of the Jacobian, passes through zero. In this case, the steady-state solution can contain a stationary shock. Such steady-states are difficult to capture numerically. Standard numerical schemes for conservation laws will, in general, fail to preserve the delicate balance between the fluxes and the source terms that is required in order to generate such states.

3. **Drain on a bottom.** Dry areas, where $h\sim 0$, resemble a state of vacuum in gas dynamics, and are hard to capture numerically. In such areas, even small numerical oscillations may result in negative value(s) of h, and then it becomes impossible to calculate the characteristic speeds, $u\pm\sqrt{gh}$. This is the reason as of why high-order upwind schemes typically fail to compute such solutions.

Numerical approximations of the Saint-Venant system (1) have recently attracted a lot of attention. LeVeque *et al.* [6, 7] proposed a method which preserves stationary steady-states. In this method, a Riemann problem is introduced in the center of each grid cell, such that the flux difference exactly cancels the source term. In order to compute the new half-cell averaged values, one has to solve a nonlinear algebraic problem. It was shown by LeVeque in [6] that there exist cases where his iterative method does not converge. A different approach, but one that is still based on rather complicated Riemann problem solvers, was taken by Gallouët *et al.* in [2]. Kinetic schemes were proved to keep a nonnegative water height, satisfy an entropy inequality and to preserve stationary steady-states. The first-order kinetic solvers were proposed by Perthame *et al.* in [1, 8]. High-order kinetic schemes seem to satisfy only part of these properties and are of a very complicated form.

In this work we present new, high-order central-upwind schemes for approximating solutions of the Saint-Venant system. We extend the Godunov-type schemes of [4] for approximating solutions of multi-dimensional systems of conservation laws to balance laws. While avoiding the need for any Riemann solvers, the major drawback of central schemes is the relatively large dissipation ($\sim \mathcal{O}((\Delta x)^{2r}/\Delta t)$) where r is a formal order of accuracy. This numerical dissipation significantly increases if the

time step, Δt, is forced to be much smaller than the spatial scale Δx, or if the solution is computed for large times as happens, for example, in steady-state computations. Semi-discrete central schemes which were recently introduced in [3, 4, 5] have a much smaller numerical dissipation ($\sim \mathcal{O}((\Delta t)^{2r-1})$) which is achieved by utilizing *local* speeds of propagation for obtaining a more precise estimate of the width of the Riemann fans, while still avoiding the need to solve Riemann problems.
Extending the schemes of [4] to equations of the type (1) requires one to pay a careful attention to the discretization of the source term in order to imitate the differential properties on the numerical level, and by that, to be able to preserve, e.g., stationary steady-state solutions.
We present new second- and third-order schemes for approximating the solutions of (1). We prove that our second-order method preserves the non-negativity of the height of the water. This is especially important when the water flows out of a certain domain, and dry states ($h \sim 0$) appear.
Our numerical simulations, in one and two space dimensions, validate the desired proprieties of our new schemes in a variety of test cases: small perturbations of steady-state solutions, transcritical flows and drainage on a non-flat bottom.

References

[1] Audusse E., Bristeau M.O., Perthame B., *Kinetic Schemes for Saint-Venant Equations With Source Terms on Unstructured Grids*, INRIA Report RR-3989, (2000).

[2] Gallouët T., Hérard J.-M., Seguin N., *Some Approximate Godunov Schemes to Compute Shallow-Water Equations with Topography*, AIAA-2001, to appear.

[3] Kurganov A., Levy D., *A Third-Order Semi-Discrete Scheme for Conservation Laws and Convection-Diffusion Equations*, SIAM J. Sci. Comp., **22**, (2000), pp.1461–1488.

[4] Kurganov A., Noelle S., Petrova G., *Semi-Discrete Central-Upwind Schemes for Hyperbolic Conservation Laws and Hamilton-Jacobi Equations*, SIAM J. Sci. Comp., **23**, (2001), pp.707–740.

[5] Kurganov A., Tadmor E., *New High-Resolution Central Schemes for Nonlinear Conservation Laws and Convection-Diffusion Equations*, J. Comput. Phys., **160**, (2000), pp.214–282.

[6] LeVeque R.J, *Balancing Source Terms and Flux Gradients in High-Resolution Godunov Methods: The Quasi-Steady Wave-Propagation Algorithm*, J. Comput. Phys., **146**, (1998), pp.346–365.

[7] LeVeque R.J., Bale D.S., *Wave Propagation Methods for Conservation Laws with Source Terms*, Hyperbolic Problems: Theory, Numerics, Applications, Vol. II (Zürich, 1998), pp. 609–618, Int. Ser. Numer. Math., 130, Birkhäuser, Basel, 1999.

[8] Perthame B., Simeoni C., *A Kinetic Scheme for the Saint-Venant System with a Source Term*, Ecole Normale Superieure Report DMA–01–13, (2001).

4.19 Tuesday, Session 4 (morning): Shock waves

Existence and Stability of Multidimensional Transonic Shocks for the Euler Equations for Potential Fluids

Gui-Qiang Chen*

Northwestern University, USA

Mikhail Feldman

University of Wisconsin at Madison, USA

In this talk we will discuss some recent results on the existence and stability of multidimensional transonic shocks for the Euler equations for steady potential fluids in infinite cylinders. The Euler equations, consisting of the conservation law of mass and the Bernoulli law for velocity, can be written as a second-order, nonlinear elliptic-hyperbolic equation of mixed type for the velocity potential. The transonic shock problem in an infinite cylinder can be formulated into the following free boundary problem: The free boundary is the location of the multidimensional transonic shock which divides two regions of smooth flow in the infinite cylinder, and the equation is hyperbolic in the upstream region where the smooth perturbed flow is supersonic. We will introduce a nonlinear approach to deal with such a free boundary problem in order to solve the transonic shock problem in unbounded domains. Our results indicate that there exists a unique solution of the free boundary problem such that the equation is always elliptic in the unbounded downstream region, the velocity state at infinity in the downstream direction is uniquely determined by the given hyperbolic phase, and the free boundary is smooth, provided that the hyperbolic phase is close to a uniform flow; and the free boundary is also stable under the steady perturbation of the hyperbolic phase. We will also present some further results in this direction, including the results on the existence and stability of multidimensional transonic shocks near spherical or circular transonic shocks in unbounded domains, if time permits.

Weak stability of multidimensional shocks

Jean-François Coulombel

École Normale Supérieure de Lyon, France

The linear stability of multidimensional shocks for systems of conservation laws was extensively studied by A. Majda in the early 80's, see [5]. The analysis was based on a uniform stability condition which is the analogue of Kreiss' condition for hyperbolic initial boundary value problems, see [3]. The linear stability results enabled A. Majda to prove the existence of multidimensional shock waves when the initial data meet the uniform stability condition, see [4]. The results of [5, 4] were later refined using Bony's paradifferential calculus, see [6]. The introduction of these new techniques precised the regularity that is sufficient to derive the energy estimates obtained by Majda.

The purpose of this talk is to show that Majda's approach can be extended to study the linear stability of weakly stable multidimensional shocks: these are discontinuities for which the uniform stability condition is violated due to the appearance of "surface"or "boundary"waves. Examples of such weakly stable shocks arise in real gas dynamics (when the isentropes are non convex in the density-pressure plane) and in the study of subsonic phase transitions in a van der Waals fluid [1]. Shock waves for a multidimensional scalar conservation law provide us with another example (unfortunately, we do not know any physical example of such equations). Moreover, our analysis does not apply to such shock waves for technical reasons (we shall briefly address this point during the talk).

We consider a general system of N conservation laws ($N \geq 2$) in the whole space $\mathbb{R}^d$ ($d \geq 2$):

$$\partial_t u + \sum_{j=1}^{d} \partial_{x_j} f_j(u) = 0 \,, \tag{1}$$

supplemented with an initial condition taking the form of a shock wave (the shock is assumed to be noncharacteristic). Following Majda, we transform this Cauchy problem in an initial boundary value problem in a fixed domain. The first part of our work consists in deriving an energy estimate for the constant coefficients linearized problem. Linearizing (1) about a planar shock wave u yields a *non classical* initial boundary value problem of the form

$$\begin{cases} \mathcal{L}_u(v) := \partial_t\, v + \displaystyle\sum_{j=1}^{d-1} \mathcal{A}_j(u)\, \partial_{x_j} v + \mathcal{A}_d(u)\, \partial_z v = f & t > 0,\, z > 0, \\ \mathcal{B}_u(\varphi, v) := \partial_t \varphi\; b_0(u) + \displaystyle\sum_{j=1}^{d-1} \partial_{x_j} \varphi\; b_j(u) + M(u)\, v = g & t > 0,\, z = 0, \end{cases} \tag{2}$$

where $v = (v_+, v_-)$ denotes the unknown function on either side of the unknown shock front and $\{x_{\,d} = \varphi(t, x_1, \ldots, x_{d-1})\}$ is the unknown shock front curve (z is a new coordinate appearing once this front has been fixed). System (2) is called a *non classical* initial boundary value problem because a partial differential equation on the shock front curve φ is coupled with the transmission problem on (v_+, v_-); the transmission relations, that are represented by the matrix $M(u)$, come from the Rankine-Hugoniot conditions. Energy estimates for (2) when u is a weakly stable shock have been derived by the author for the two first examples mentioned above, see [2]. We shall here present the general hypotheses that yield a similar result; under these "generic"assumptions, we shall show that suitable modifications in Kreiss' symmetrizer construction yield a symbolic symmetrizer $R(\xi)$ for the initial boundary value problem (2) and, as a consequence, the energy estimate. The symbolic symmetrizer $R(\xi)$ takes the form of a Fourier multiplier in the constant coefficients case. Recall first that energy estimates for initial boundary value problems are obtained by making a Laplace transform in the variable t. This amounts to work with the new unknown functions

$$(\Phi, V) = (e^{-\gamma t}\varphi, e^{-\gamma t} v)\,, \quad t \in \mathbb{R}\,,$$

where γ is a nonnegative number. We now look for functions (Φ, V) defined for all values of t and solutions to the system

$$\begin{cases} \mathcal{L}_u^\gamma(V) := \mathcal{L}_u(V) + \gamma V = e^{-\gamma t} f & z > 0, \\ \mathcal{B}_u^\gamma(\Phi, V) := \mathcal{B}_u(\Phi, V) + \gamma \Phi\; b_0 = e^{-\gamma t} g & z = 0. \end{cases} \tag{3}$$

When the planar shock u satisfies the uniform stability condition, energy estimates for system (3) can be obtained in Sobolev spaces with appropriate weighted norms. Functions defined in the interior domain

$$\Omega := \{(t, x_1, \ldots, x_{d-1}, z) \in \mathbb{R} \times \mathbb{R}^d \,/ z > 0\}$$

are estimated in the Sobolev space $H^k(\Omega)$ (with norm $\| \cdot \|\|\|_{\|} k, \gamma$) and functions defined on the boundary $\omega = \partial\Omega$ are estimated in the Sobolev space $H^m(\omega)$ (with norm $\| \cdot \|_{m,\gamma}$). We refer to [5, 6] for the precise definitions of the norms. The energy estimate derived in [5] under the uniform stability condition reads

$$\gamma \|V\|\|\|_{\|} 0, \gamma^2 + \|V\|_{0,\gamma}^2 + \|\Phi\|_{1,\gamma}^2 \leq C \left(\frac{1}{\gamma} \|\mathcal{L}\|_u^\gamma V \|_{\|} 0, \gamma^2 + \|\mathcal{B}_u^\gamma(\Phi, V)\|_{0,\gamma}^2 \right)\,. \tag{4}$$

When the shock u violates the uniform stability condition but meets our "weak stability"assumption, we shall show that solutions of (3) satisfy an energy estimate of the form

$$\gamma \|V\|\|\|_{\|} 0, \gamma^2 + \|V\|_{0,\gamma}^2 + \|\Phi\|_{1,\gamma}^2 \leq C \left(\frac{1}{\gamma^3} \|\mathcal{L}\|_u^\gamma V \|_{\|} 1, \gamma^2 + \frac{1}{\gamma^2} \|\mathcal{B}_u^\gamma(\Phi, V)\|_{1,\gamma}^2 \right)\,. \tag{5}$$

This is the extension to a general framework of the results obtained in [2]. It includes Majda's proposition about weakly stable shock waves for real gas dynamics [5].

The second part of our work is the application of this preliminary result to the variable coefficients linearized system. The state $\widetilde{u}$ about which the system of conservation laws (1) is linearized is now a compactly supported perturbation of the planar shock u, such that $\widetilde{u}$ defines a weakly stable shock. Performing our modified Kreiss' symmetrizer construction (after freezing the coefficients), we obtain a global symbolic symmetrizer $R(t, \mathbf{x}, \xi)$ (with $\mathbf{x} = (x_1, \ldots, x_{d-1}, z)$) whose regularity in the variables $(t, \mathbf{x})$ is governed by the regularity of $\widetilde{u}$. Using a parameter version of Bony's paradifferential calculus as in [6], we show that the energy estimate (3) is still valid under some appropriate assumptions on the regularity of $\widetilde{u}$. This extends Majda's linear results to weakly stable shocks that meet our assumptions.

References

[1] S. Benzoni-Gavage. Stability of multi-dimensional phase transitions in a van der Waals fluid. *Nonlinear Anal.*, 31(1-2):243–263, 1998.

[2] J. F. Coulombel. Weak stability of non uniformly stable multidimensional shocks. *submitted to SIAM J. Math. Anal.*

[3] H. O. Kreiss. Initial boundary value problems for hyperbolic systems. *Comm. Pure Appl. Math.*, 23:277–298, 1970.

[4] A. Majda. The existence of multidimensional shock fronts. *Mem. Amer. Math. Soc.*, 43(281):v+93, 1983.

[5] A. Majda. The stability of multidimensional shock fronts. *Mem. Amer. Math. Soc.*, 41(275):iv+95, 1983.

[6] G. Métivier. Stability of multidimensional shocks. In *Advances in the theory of shock waves*, pages 25–103. Birkhäuser, 2001.

Propagation and interaction of delta-shock waves

V. G. Danilov

Moscow Technical University of Communication and Informatics, Russia

V. M. Shelkovich*

St.-Petersburg State Architecture and Civil Engineering University, Russia

1. In [1]– [4] *the weak asymptotics method* was developed. This method enables an investigation of *the dynamics of propagation and interaction* of various types of nonlinear waves concerned with quasilinear hyperbolic systems of conservation laws. It was used to study shock waves and infinitely narrow solitons. Here *a modified weak asymptotics method* is applied to the case of *delta-shock waves*. We consider the system

$$\begin{aligned} L_1[u] = u_t + \big(f(u)\big)_x &= 0, \\ L_2[u,v] = v_t + \big(g(u)v\big)_x &= 0, \end{aligned} \tag{1}$$

where $f(u)$, $g(u)$ are smooth functions, $f''(u) > 0$, $g'(u) > 0$, $f'(u) \le g(u)$ (see [5]– [9]), $u = u(x,t), v = v(x,t) \in \mathbb{R}$, $x \in \mathbb{R}$. The initial value is

$$\begin{aligned} u^0(x) &= u_0 + \textstyle\sum_{k=1}^2 u_k H(-x + x_k^0), \\ v^0(x) &= v_0 + \textstyle\sum_{k=1}^2 \big(v_k H(-x + x_k^0) + e_k^0 \delta(-x + x_k^0)\big), \end{aligned} \tag{2}$$

where $H(x)$ is the Heaviside function, $\delta(x)$ is the Dirac delta function, u_0, $u_k > 0$, v_0, v_k, e_k^0 are constants, $k = 1, 2$, $x_1^0 < x_2^0$. Here, unlike some well known papers, the initial value may contain δ-functions (solutions in the standard form of delta-shock waves are obtained if we set $e_1^0 = e_2^0 = 0$).
We consider the problem of *propagation* of delta-shock waves for system (1) and the problem of *interaction* of two delta-shock waves for the system

$$\begin{aligned} L_{01}[u] = u_t + (u^2/2)_x &= 0, \\ L_{02}[u,v] = v_t + (uv)_x &= 0. \end{aligned} \tag{3}$$

To obtain a solution in the form of delta-shock waves the parabolic regularization and the Dafermos–DiPerna regularization of systems, the Colombeau theory, the Lax formula, and Volpert's product are used (see [5]– [9]). In the framework of our approach, roughly speaking, we consider *all regularizations* of delta-shock type solutions to the above systems (see Definitions 1, 2).

2. To study propagation of *one* delta-shock wave we must solve the Cauchy problem (1), (2), where we set $u_2 = v_2 = 0$ or $u_2 = v_2 = e_2^0 = 0$. In this case we must seek a solution in the form of the singular ansatz

$$\begin{aligned} u(x,t) &= u_0 + u_1 H(-x+\phi(t)), \\ v(x,t) &= v_0 + v_1 H(-x+\phi(t)) + e(t)\delta(-x+\phi(t)), \end{aligned} \tag{4}$$

where $e(t)$, $\phi(t)$ are functions to be found.
To find the solution in the form (4) we construct the smooth ansatz (which is a smooth regularization of (4)):

$$\begin{aligned} u(x,t,\varepsilon) &= u_0 + u_1 H_u(-x+\phi(t),\varepsilon) + R\Omega\big(\tfrac{-x+\phi(t)}{\varepsilon}\big), \\ v(x,t,\varepsilon) &= v_0 + v_1 H_v\big(-x+\phi(t),\varepsilon\big) + e(t)\delta_v\big(-x+\phi(t),\varepsilon\big), \end{aligned} \tag{5}$$

where R is a constant, $H_j(x,\varepsilon) = \omega_{0j}\big(\frac{x}{\varepsilon}\big) = \int_{-\infty}^{\frac{x}{\varepsilon}} \tilde\omega_j(\eta)\,d\eta$ are regularizations of the Heaviside function $H(x)$, $j = u, v$, $\delta_v(x,\varepsilon) = \frac{1}{\varepsilon}\omega_v\big(\frac{x}{\varepsilon}\big)$ and $\frac{1}{\varepsilon}\Omega\big(\frac{x}{\varepsilon}\big)$ are regularizations of the δ-function. Here the mollifiers $\tilde\omega_u(\eta)$, $\tilde\omega_v(\eta)$, $\omega_v(\eta)$, $\Omega(\eta)$ have the following properties: $0 \le \omega(\eta) \in C^\infty(\mathbb{R})$, $\omega(-\eta) = \omega(\eta)$, $\int \omega(\eta)\,d\eta = 1$, $\omega(\eta)$ has a compact support or decreases sufficiently rapidly as $|\eta| \to \infty$.

Definition 1 The smooth ansatz (5) is called *admissible* for the Cauchy problem (1), (2) (where $u_2 = v_2 = 0$ or $u_2 = v_2 = e_2^0 = 0$) if

$$\frac{f(u_0+u_1) - f(u_0)}{u_1} = \int g\Big(u_0 + u_1\omega_{0u}(\eta) + R\Omega(\eta)\Big)\omega_v(\eta)\,d\eta. \tag{6}$$

If $f(u) = u^2/2$, $g(u) = u$ relation (7) has the form

$$R = \frac{u_1(1-2a)}{2b},$$

where $a = \int \omega_{0u}(\eta)\omega_v(\eta)\,d\eta$, $b = \int \Omega(\eta)\omega_v(\eta)\,d\eta$.

Definition 2 The *admissible* smooth ansatz (5) is called a *generalized asymptotic* delta-shock wave type solution of the Cauchy problem (1), (2) for $t \in [0,\ T]$ if

$$\begin{aligned} L_1[u(x,t,\varepsilon)] &= O_{\mathcal{D}'}(\varepsilon), \\ L_2[u(x,t,\varepsilon), v(x,t,\varepsilon)] &= O_{\mathcal{D}'}(\varepsilon), \\ u(x,0,\varepsilon) &= u^0(x) + O_{\mathcal{D}'}(\varepsilon), \\ v(x,0,\varepsilon) &= v^0(x) + O_{\mathcal{D}'}(\varepsilon), \end{aligned}$$

where the first and second estimates are uniform with respect to $t \in [0,\ T]$. By $O_{\mathcal{D}'}(\varepsilon^\alpha)$ we denote a distribution from $\mathcal{D}'(\mathbb{R})$ such that

$$\langle O_{\mathcal{D}'}(\varepsilon^\alpha), \varphi(x)\rangle = O(\varepsilon^\alpha), \quad \forall\varphi(x) \in \mathcal{D}(\mathbb{R})$$

and $O(\varepsilon^\alpha)$ is understood in the ordinary sense.

Definition 3 Let (5) be a generalized asymptotic solution of the Cauchy problem (1), (2). By a *generalized solution* of the Cauchy problem (1), (2) for $t \in [0,\ T]$ we call the weak limit

$$\begin{aligned} u(x,t) &= \lim\nolimits_{\varepsilon\to+0} u(x,t,\varepsilon), \\ v(x,t) &= \lim\nolimits_{\varepsilon\to+0} v(x,t,\varepsilon). \end{aligned}$$

Theorem 1 *The Cauchy problem* (1), (2), *where* $u_2 = v_2 = 0$, *for* $t \in [0,\ \infty)$ *has a unique generalized solution* (4) *if and only if,*

$$\begin{aligned} \phi(t) &= \tfrac{[f(u)]}{[u]}t, \\ e(t) &= e^0 + \Big([g(u)v] - \tfrac{[f(u)]}{[u]}[v]\Big)t, \end{aligned} \tag{7}$$

where $[v] = v_1$, $[u] = u_1$, $[f(u)] = f(u_0+u_1) - f(u_0)$, $[g(u)v] = g(u_0+u_1)(v_0+v_1) - g(u_0)v_0$ *are jumps in functions* v, u, $f(u)$, $g(u)v$ *across the discontinuity line* $x = \phi(t)$.

In the framework of our approach the substitution of the singular ansatz means that the *admissible* smooth ansatz (5) is substituted into (1) and the weak asymptotics of the left-hand side of the system is found up to $O_{\mathcal{D}'}(\varepsilon)$. In order to construct this weak asymptotics we use the results obtained in [2]– [4]):

$$f\big(u(x,t,\varepsilon)\big) = f(u_0) + \Big(f(u_0+u_1) - f(u_0)\Big)H(-x+\phi(t)) + O_{\mathcal{D}'}(\varepsilon), \quad \varepsilon \to +0, \tag{8}$$

$$\begin{aligned} v(x,t,\varepsilon)g\big(u(x,t,\varepsilon)\big) = g(u_0)v_0 + \Big(g(u_0+u_1)(v_0+v_1) - g(u_0)v_0\Big)H(-x+\phi(t)) \\ +\Lambda e(t)\delta(-x+\phi(t)) + O_{\mathcal{D}'}(\varepsilon), \quad \varepsilon \to +0, \end{aligned} \tag{9}$$

where $\Lambda = \int g\big(u_0 + u_1\omega_{0u}(\eta) + R\Omega(\eta)\big)\omega_v(\eta)\,d\eta$.
Substituting (8), (9) into the left-hand side of system (1), *separating singularities* and using Definitions 2, 3, we obtain system (7) and the relation (6).

Remark 4.1 Without introducing the term $R\Omega(\frac{-x+\phi(t)}{\varepsilon})$, we cannot solve the Cauchy problem with an *arbitrary initial value* (2). It follows that to construct solution (4) of the Cauchy problem we must use only *the admissible* ansatz (5) whose mollifiers and R are connected with the initial value (2) by relation (6). In this case, we may define R from relation (6) for *any initial value*. However solution (4) itself *does not depend* on this relation (see (7)).

3. We consider the problem of interaction for system (3). In order to investigate the interaction of *two* delta-shock waves, that is, to solve the Cauchy problem (3), (2) we should seek a solution in the form of the singular ansatz

$$\begin{aligned} u(x,t) &= u_0 + \textstyle\sum_{k=1}^2 u_k H(-x+\phi_k(t)), \\ v(x,t) &= v_0 + \textstyle\sum_{k=1}^2 \Big(v_k H(-x+\phi_k(t)) + e_k(t)\delta(-x+\phi_k(t))\Big), \end{aligned} \tag{10}$$

where $e_k(t)$, $\phi_k(t)$ are functions to be found.
The smooth ansatz connected with the singular ansatz (10) has the form

$$\begin{aligned} u(x,t,\varepsilon) &= u_0 + \textstyle\sum_{k=1}^2 \Big(u_k H_{uk}\big(-x+\phi_k(t,\varepsilon),\varepsilon\big) + R_k(t,\varepsilon)\Omega_k'\big(\frac{-x+\phi(t)}{\varepsilon}\big)\Big), \\ v(x,t,\varepsilon) &= v_0 + \textstyle\sum_{k=1}^2 \Big(v_k H_{vk}\big(-x+\phi_k(t,\varepsilon),\varepsilon\big) + e_k(t,\varepsilon)\delta_{vk}\big(-x+\phi_k(t,\varepsilon),\varepsilon\big)\Big), \end{aligned} \tag{11}$$

where $H_{jk}(x,\varepsilon) = \omega_{0jk}\big(\frac{x}{\varepsilon}\big) = \int_{-\infty}^{\frac{x}{\varepsilon}} \tilde{\omega}_{jk}(\eta)\,d\eta$ are regularizations of the Heaviside function $H(x)$, $\delta_{vk}(x,\varepsilon) = \frac{1}{\varepsilon}\omega_{\delta k}\big(\frac{x}{\varepsilon}\big)$ and $\frac{1}{\varepsilon}\Omega_k\big(\frac{x}{\varepsilon}\big)$ are regularizations of the δ-function, $j = u, v$, $k = 1, 2$. Here $R_k(t,\varepsilon)$ and $\frac{dR_k(t,\varepsilon)}{dt}$ are bounded functions for all $t \ge 0$ and for all $\varepsilon \in [0,\,\varepsilon_0)$, $\varepsilon_0 > 0$.
Now we outline the construction of the *generalized asymptotic* solution (11) in the sense of Definition 2.
If $t \in [0,\ t^*)$, where $t = t^* > 0$ is time of the interaction, we have two delta-shock waves propagating without interaction. By Theorem 1, their phases $\phi_{k0}(t)$ and the amplitudes of delta-functions $e_{k0}(t)$, $k = 1, 2$ satisfy the system of equations

$$\begin{aligned} \phi_{10}(t) &= \phi_{10}(0) + \tfrac{[u^2/2]_1}{[u]_1}t = \phi_{10}(0) + (u_0 + u_1/2 + u_2)t, \\ \phi_{20}(t) &= \phi_{20}(0) + \tfrac{[u^2/2]_2}{[u]_2}t = \phi_{20}(0) + (u_0 + u_2/2)t, \\ e_{10}(t) &= e_{10}(0) + \Big([uv]_1 - \tfrac{[u^2/2]_1}{[u]_1}[v]_1\Big)t = e_{10}(0) + \tfrac{1}{2}u_1(2v_0 + v_1 + 2v_2)t, \\ e_{20}(t) &= e_{20}(0) + \Big([uv]_2 - \tfrac{[u^2/2]_2}{[u]_2}[v]_2\Big)t = e_{20}(0) + \tfrac{1}{2}u_2(2v_0 + v_2)t, \end{aligned} \tag{12}$$

where $\phi_{k0}(0) = x_k^0$, $e_{10}(0) = e_k^0$, $k = 1, 2$. Here the *time of interaction* $t = t^* > 0$ is defined as a root of the equation $\psi_0(t^*) = 0$, where $\psi_0(t) = \phi_{20}(t) - \phi_{10}(t) = \phi_{20}(0) - \phi_{10}(0) - (u_1 + u_2)t/2$ is the distance between the fronts of non-interacting delta-shock waves.
In order to *describe the interaction dynamics* we will seek the phases $\phi_k(t,\varepsilon)$ and amplitudes $e_k(t,\varepsilon)$ as functions of the fast variable $\tau \in \mathbb{R}$ and the slow variable $t \ge 0$:

$$\begin{aligned} \phi_k(t,\varepsilon) \stackrel{def}{=} \widehat{\phi}_k(\tau,t) &= \phi_{k0}(t) + \psi_0(t)\phi_{k1}(\tau), \\ e_k(t,\varepsilon) \stackrel{def}{=} \widehat{e}_k(\tau,t) &= e_{k0}(t) + \psi_0(t)e_{k1}(\tau), \end{aligned} \tag{13}$$

where the functions $\phi_{k0}(t)$ *are extended by the same equations* (12) for all $t \in [t^*,\ +\infty)$.

It is clear that *before interaction* ($t < t^*$), we have $\tau > 0$; *after interaction* ($t > t^*$) we have $\tau < 0$. Therefore, we set the following boundary conditions for the perturbations:

$$\begin{array}{rclrcl} \phi_{k1}(\tau)\Big|_{\tau\to+\infty} &=& 0, & e_{k1}(\tau)\Big|_{\tau\to+\infty} &=& 0, \\ \frac{d\phi_{k1}(\tau)}{d\tau}\Big|_{\tau\to-\infty} &=& o(\tau^{-1}), & \frac{de_{k1}(\tau)}{d\tau}\Big|_{\tau\to-\infty} &=& o(\tau^{-1}). \end{array} \tag{14}$$

Finding the limit values of the perturbations as $\tau \to -\infty$

$$\phi_{k1}(\tau)\Big|_{\tau\to-\infty} = \phi_{k1,-}, \qquad e_{k1}(\tau)\Big|_{\tau\to-\infty} = e_{k1,-}, \quad k = 1, 2,$$

we *determine "the result"* of the interaction for $t > t^*$.
One can obtain the following asymptotic expansions analogous to (8), (9):

$$\begin{array}{rcl} H_{u1}(-x,\varepsilon)H_{u2}(-x+a,\varepsilon) &=& B_1\big(\frac{a}{\varepsilon}\big)H(-x) + \Big(1 - B_1\big(\frac{a}{\varepsilon}\big)\Big)H(-x+a) + O_{\mathcal{D}'}(\varepsilon), \\ H_{u1}(-x,\varepsilon)\delta_{v2}(-x+a,\varepsilon) &=& \Big(1 - B_1^{u1,\delta 2}(\rho)\Big)\delta(-x+a) + O_{\mathcal{D}'}(\varepsilon), \quad \varepsilon \to +0, \end{array} \tag{15}$$

where the estimate $O_{\mathcal{D}'}(\varepsilon)$ is uniform with respect to a,

$$B_1(\rho) = \int_{-\infty}^{\rho} \big(\check{\tilde{\omega}}_{u1} * \tilde{\omega}_{u2}\big)(\eta)\,d\eta, \qquad B_1^{u1,\delta 2}(\rho) = \int_{-\infty}^{\rho} \big(\tilde{\omega}_{u1} * \check{\omega}_{v2}\big)(\eta)\,d\eta \tag{16}$$

are *interaction switch functions*, $\check{\omega}(\eta) = \omega(-\eta)$, $*$ is the operation of convolution.
Substituting (13), (8), (9), (15) into (2) we have, up to $O_{\mathcal{D}'}(\varepsilon)$ for all $t \geq 0$ and $\tau \in \mathbb{R}$

$$\begin{array}{rcl} \frac{d\phi_{10}(t)}{dt} + \frac{d\psi_0(t)}{dt}\frac{d}{d\tau}\Big(\tau\phi_{11}(\tau)\Big) &=& u_0 + u_1/2 + u_2 B_1(\rho), \\ \frac{d\phi_{20}(t)}{dt} + \frac{d\psi_0(t)}{dt}\frac{d}{d\tau}\Big(\tau\phi_{21}(\tau)\Big) &=& u_0 + u_2/2 + u_1\Big(1 - B_1(\rho)\Big), \end{array} \tag{17}$$

$$\begin{array}{rcl} \frac{de_{10}(t)}{dt} + \frac{d\psi_0(t)}{dt}\frac{d}{d\tau}\Big(\tau e_{11}(\tau)\Big) &=& u_1v_0 + u_1v_1/2 + u_1v_2B_1^{u1,v2}(\rho) \\ && +u_2v_1B_1^{v1,u2}(\rho) - v_1u_2B_1(\rho), \\ \frac{de_{20}(t)}{dt} + \frac{d\psi_0(t)}{dt}\frac{d}{d\tau}\Big(\tau e_{21}(\tau)\Big) &=& u_2v_0 + u_2v_2/2 + u_1v_2\Big(1 - B_1^{u1,v2}(\rho)\Big) \\ && +u_2v_1\Big(1 - B_1^{v1,u2}(\rho)\Big) - v_2u_1\Big(1 - B_1(\rho)\Big), \end{array} \tag{18}$$

where $B_1^{u1,v2}(\rho) = \int_{-\infty}^{\rho} \big(\check{\tilde{\omega}}_{u1} * \tilde{\omega}_{v2}\big)(\eta)\,d\eta$, $B_1^{v1,u2}(\rho) = \int_{-\infty}^{\rho} \big(\check{\tilde{\omega}}_{v1} * \tilde{\omega}_{u2}\big)(\eta)\,d\eta$ are *interaction switch functions*.
Here

$$\rho(\tau) = \frac{\phi_2(t,\varepsilon) - \phi_1(t,\varepsilon)}{\varepsilon} \stackrel{def}{=} \tau\big(1 + \phi_{21}(\tau) - \phi_{11}(\tau)\big)$$

satisfies the differential equation

$$\begin{array}{rcl} \frac{d\rho}{d\tau} &=& F(\rho) = 2B_1(\rho) - 1, \\ \frac{\rho(\tau)}{\tau}\Big|_{\tau\to+\infty} &=& 1, \end{array} \tag{19}$$

where the boundary condition (19) follows from (14).
All *interaction switch functions* have the following limit properties: they tend to 1 as $\rho \to +\infty$ and they tend to 0 as $\rho \to -\infty$ (see [3], [4]). Taking into account these properties for all $t \in (0,\ t^*)$ as $\tau \to -\infty$, we derive from (17), (18), (14) the system (12) which describes the dynamics of propagation of two delta-shock waves *before their interaction* for $t < t^*$.
Since the equation $F(\rho) = 0$ has a root ρ_0 which satisfies the equation $B_1(\rho) = 1/2$, we have $\rho = \tau\big(1+\phi_{21}(\tau)-\phi_{11}(\tau)\big) \to \rho_0$ as $\tau \to -\infty$ and $B_k\big((-1)^{k-1}\rho\big) \to B_k((-1)^{k-1}\rho_0) = 1/2$, $k = 1, 2$. Thus, passing to the limit in system (17) as $\tau \to -\infty$, we obtain the system of equations which describes the phases of delta-shock waves *after interaction* for $t > t^*$:

$$\begin{array}{rcl} \frac{d\widehat{\phi}_{1,-}(t)}{dt} &=& \frac{d\phi_{10}(t)}{dt} + \frac{d\psi_0(t)}{dt}\phi_{11,-} = u_0 + u_1/2 + u_2/2, \\ \frac{d\widehat{\phi}_{2,-}(t)}{dt} &=& \frac{d\phi_{20}(t)}{dt} + \frac{d\psi_0(t)}{dt}\phi_{21,-} = u_0 + u_2/2 + u_1/2, \end{array} \tag{20}$$

where $\widehat{\phi}_{k,-}(t^*) = \phi_{k0}(t^*) = x^*$. It can be seen that the phase limit values of both delta-shock waves *coincide* ($\widehat{\phi}_{2,-}(t) = \widehat{\phi}_{1,-}(t) \stackrel{def}{=} \widehat{\phi}_-(t)$) and hence after the interaction these delta-shock waves *merge into one*.
Using the *asymptotic generalized* solution (11) constructed above, we obtain a *generalized solution* (10) in the sense of Definition 3.

Theorem 2 *The Cauchy problem* (3), (2) *for all* $t \in [0, +\infty)$ *has a generalized solution* (10), *where*

$$\begin{aligned} \phi_k(t) &= x_k^0 + \frac{[u^2/2]_k}{[u]_k} t + (-1)^k \cdot \frac{u_{3-k}}{2} \cdot (t-t^*)H(t-t^*), \\ e_k(t) &= e_k^0 + \Big([uv]_k - \frac{[u^2/2]_k}{[u]_k}[v]_k\Big)t + (-1)^k \cdot \frac{u_k v_{3-k}}{2} \cdot (t-t^*)H(t-t^*), \quad k=1,2. \end{aligned} \tag{21}$$

Thus, for $t \in (0,\ t^*)$ we have *two* delta-shock waves which after interaction (at the instant $t = t^*$) merge constituting *one* new delta-shock wave (see (20)). Here, the functions $\frac{de_{k0}(t)}{dt}$ have the jumps $(-1)^k \cdot \frac{u_k v_{3-k}}{2}$, $k = 1, 2$.

References

[1] V. M. Shelkovich. An associative-commutative algebra of distributions that includes multiplicators, generalized solutions of nonlinear equations, Math. Notices, 1995, v. 57, No 5, 765–783.

[2] V. G. Danilov, V. P. Maslov, V. M. Shelkovich. Algebra of singularities of singular solutions to first-order quasilinear strictly hyperbolic systems, Theor. Math. Phys., 1998, v. 114, No 1, 1–42.

[3] V. G. Danilov, V. M. Shelkovich, Propagation and interaction of nonlinear waves, Eighth International Conference on Hyperbolic prorblems. Theory–Numerics–Applications, Magdeburg, Germany, February 28–March 3, 2000, 326–328.

[4] V. G. Danilov and V. M. Shelkovich, Propagation and interaction of shock waves of quasilinear equation, Nonlinear Studies, 2001, v. 8, No. 1, 135–170.

[5] Philippe Le Floch, An existence and uniqueness result for two nonstrictly hyperbolic systems, Nonlinear Evolution Equations That Change Type, Springer-Verlag, 1990, 126–138.

[6] Dechun Tan, Tong Zhang and Yuxi Zheng, Delta-shock waves as limits of vanishing viscosity for hyperbolic systems of conservation laws, J. Diff. Eqns., 1994, v. 112, 1–32.

[7] B. Lee Keyfitz and H. C. Kranzer, Spaces of Weighted Measures for Conservation Laws with Singular Shock Solutions, J. Diff. Eqns., 1995, v. 118, 420–451.

[8] G. Ercole, Delta-shock waves as self-similar viscosity limits, Ouart. Appl. Math, 2000, v. LVIII, No 1, 177–199.

[9] Marko Nedeljkov, Delta and singular delta locus for one dimensional systems of conservation laws, Preprint ESI 837, Vienna, 2000.

4.20 Tuesday, Session 4 (afternoon): Numerical methods I

Kinematic and Dynamic Dissipation in Shock Capturing Schemes

Kun Xu

Hong Kong University of Science and Technology, China

In order to represent a physical solution in a discretized space, the numerical representation depends closely on the relative scales of the mesh size and the physical flow structure. For a solution determined by the physical viscosity μ_{phys}, its numerical representation depends on the mesh size Δx used. If the mesh size is much smaller than the thickness of the physical structure l_p, i.e. $\Delta x << l_p$, any consistent scheme should give an accurate solution. However, with the use of a coarse mesh, i.e., $\Delta x > l_p$, phenomena which are not included in the original physical solution appear. Two considerations have to be taken into account correctly to represent the numerical fluid with coarse mesh.
(i). the physical structure l_p is replaced by a numerical one with the thickness of the cell size Δx.
(ii) there appears discontinuities at the cell interface.
In the CFD algorithm development, these two factors have been considered separately. Two classical pioneering papers for the shock capturing schemes are by von Neumann $\&$ Richtmyer and by Godunov. von Neumann $\&$ Richtmyer realized the factor (i) and compensated for it by requiring additional numerical dissipation in the governing equations, which would enlarge the shock thickness to the scale of the cell size. As a result, the governing equation for the numerical fluid should be a viscous governing equation and the total dissipation includes two parts, $\mu_{total} = \mu_{phys} + \mu_{num}$. This amount of numerical dissipation μ_{num} which is included in the governing equations is defined as **dynamic** dissipation. Following the original idea of von Neumann and Richtmyer, a number of different artificial dissipative terms have been tried by various authors. It is still an active research area to design a general dependence of μ_{num} on the flow distribution.
The success of the Godunov method is that it realizes the factor (ii), which introduces a discontinuity at the cell interface in the flow representation. The introduction of a discontinuity become paramountly important, because it associates with the implicit dissipation due to the non-conservation of the total kinetic energy in the averaging process. The dissipation introduced through the conversion of kinetic energy into thermal one in the initial data can be hardly recovered dynamically through a modification of the governing equation. Since the Godunov dissipation is coming purely from the initial data, we will call it as the **kinematic** dissipation. The introduction of the discontinuities also leds naturally to the incorporation of wave propagation into the numerical scheme, the so-called Riemann solution. If an exact Riemann solution is used in the flux evaluation, it could totally ignore the factor (i). In other words, even though the Godunov method captures the shock properly, but the shock thickness is obtained from the kinematic dissipation alone, which depends closely on the relative orientation of flow structure and the mesh construction. The shock instabilities can be generated in the Godunov method when the kinematic dissipation is the only source for its shock structure construction. The detail analysis and examples will be presented in the talk. For many approximate Riemann solvers, due to the different wave modeling in the gas evolution stage, the real governing equation underlying the flux construction are different from the inviscid Euler equations. For example, the KFVS and FVS schemes have a dynamic dissipation $\mu_{num} \sim \Delta t$ in the gas evolution stage. Therefore, the factor (i) is implicitly included also in the FVS methods, and the robustness of these schemes is well established. But, on the other hands, the dynamic dissipation in FVS is implicit and therefore uncontrollable. It will become a hidden harmful factor for the viscous flow simulation.
With the introduction of dynamic and kinematic dissipation, we may analyze the validity of using a generalized Riemann solver in a shock capturing scheme. For a second order scheme with high-order initial interpolation, even with a discontinuity at a cell interface the kinematic dissipation introduced in the initial data could be on the order of $\mu_{num} \sim \Delta x^2$, which is theoretically not enough to construct a numerical shock thickness which requires $\mu_{total} \sim \Delta x$. Therefore, *if a generalized Riemann problem (GRP) is precisely solved for the inviscid Euler in the gas evolution stage from the linearly distributed flow variables, where the dynamic dissipation is zero, a high-order accurate scheme could not properly capture the numerical shock waves.* Even with a discontinuity at a cell interface, additional dynamic dissipation is needed.
The current successful CFD algorithm design principles for the compressible flow are mainly based on the concepts of Total Variation Diminishing (TVD). With the definition, $TV(u^n) = \sum_j |u^n_{j+1} - u^n_j|$, the TVD condition says $TV(u^{n+1}) \leq TV(u^n)$. It is well known that the TVD method is applicable only to those problems of gas dynamics for which it is known *a priori* that their solutions meet the TVD requirement, such as the linear system or the scalar equation. For such a system, the TVD concept becomes an indispensable tool to justify the shock capturing schemes. For a nonlinear system without TVD properties in its solution, the TVD concept can be applicable truthfully to the initial data reconstruction only, such as $TV(\bar{u}^n) \leq TV(u^n)$,

where u are the cell averaged data and $\bar{u}$ are the reconstructed one. This requirement is similar to the reconstruction technique used in the MUSCL scheme to avoid the creation of local extremes. After the initial reconstruction, the flux across a cell interface is determined from the governing equation, which is basically fixed once the initial interpolated data is given. So, it seems impossible to design a scheme based on the requirement of its output result in the next time level. Therefore, for the nonlinear system, besides the TVD requirement in the initial data reconstruction, the use of dynamic and kinematic dissipation in the algorithm development becomes necessary. In order to make these concepts clear, let's consider the following example. For the Euler equations, with the initial cell averaged conservative variables w_j^n inside each cell, we can reconstruct the initial data simply by connecting the cell averaged data w_j^n at each cell center. The reconstructed continuous data satisfy the TVD property, such as

$$TV(\bar{w}^n) = TV(w^n),$$

where $TV(\bar{w}^n) = \int |\bar{w}'| dx$ and $TV(w^n) = \sum |w_{j+1}^n - w_j^n|$, and there is no local extreme created. Note that w represents the mass, momentum and energy respectively. After the above initial reconstruction, a conservative scheme in 1D case can be constructed as,

$$w_j^{n+1} = w_j^n + \int_{t^n}^{t^{n+1}} (F_{j-1/2}(t) - F_{j+1/2}(t)) dt,$$

where the numerical flux $F_{j+1/2}$ is obtained based on the reconstructed initial data $\bar{w}^n$ and the gas evolution model. Since the flow variables are continuous across each cell interface initially, within a short time step with CFL number less than 0.5, before the waves generated from the corners at the cell center propagate to the cell interface, the Lax-Wendroff gas evolution model is actually an accurate second-order Generalized Riemann Solver. The time-dependent flow variable $\bar{w}_{j+1/2}(t)$ at the cell interface can be obtained as

$$\bar{w}_{j+1/2}(t) = \bar{w}_{j+1/2}(0) + t \frac{\partial \bar{w}}{\partial t}|_{t=0}, \tag{1}$$

where the time derivative of the conservative variables can be evaluated using the reconstructed spatial derivatives. Then, the numerical flux $F_{j+1/2}(t)$ can be obtained from $\bar{w}_{j+1/2}(t)$. Since the initial data satisfy the TVD property for all conservative variables and the gas evolution stage is based on an almost exact Generalized Riemann Solver for the Euler Equations, the numerical results are supposed to be reasonable. But, numerically will find oscillatory results. This observation can be hardly explained from the TVD concept alone. Based on the dynamic and kinematic dissipation, we can explain the observation in the following, (a). even with the TVD property in the initial data reconstruction, the kinematic dissipation becomes $\mu_{num} \sim (\Delta x)^2$. (b). in the gas evolution stage, the Euler equations are precisely solved without introducing any dynamic dissipation. As a result, the total dissipation is not enough to construct a smooth shock transition, which requires $\mu \sim \Delta x$ in the shock region. The numerical behavior for the Flux Vector Splitting schemes will also be analyzed in the talk.

A Flux-Split Algorithm Applied to Conservative Models for Multicomponent Compressible Flows

Antonio Marquina* and Pep Mulet

University of Valencia, Spain

In this paper we consider a conservative model based on a level set equation introduced by Mulder, Osher and Sethian in [3], coupled to the Euler equations for gas dynamics to describe a two-component compressible flow in cartesian coordinates. It is well-known that classical shock-capturing schemes applied to conservative models are oscillatory near the interface between the two gases. Several authors have addressed this problem proposing either a primitive nonconservative algorithm, (Karni, [2]) or Lagrangian ingredients, (Ghost Fluid Method by Fedkiw, Aslam, Merriman and Osher, ([4]).
In this paper, we solve directly the conservative model by reformulating a flux-split algorithm, due to the first author, (see Donat and Marquina, [1]).
Let us consider the one dimensional Euler equations of gas dynamics

$$\mathbf{u} = (\rho, M, E)^T, \mathbf{f}(\mathbf{u}) = q\mathbf{u} + (0, P, qP) \tag{1}$$

where ρ,q,M,E and P are the density, velocity, moment, energy and pressure, respectively, where

$$E = \rho\epsilon + \frac{\rho q^2}{2} \tag{2}$$

where ϵ is the especific internal energy and the system is closed with the equation of state, (EOS), which is written as $P = P(\rho, \epsilon)$ or $P = P(\rho, T)$, being T the temperature. Since

$$\epsilon = \epsilon(\rho, T)$$

we can write

$$d\epsilon = \left.\frac{\partial \epsilon}{\partial \rho}\right|_T d\rho + \left.\frac{\partial \epsilon}{\partial T}\right|_\rho dT \tag{3}$$

which is equivalent to

$$d\epsilon = \left(\frac{P - Tp_T}{\rho^2}\right) d\rho + c_v dT \tag{4}$$

where c_v is the specific heat at constant volume. The local sound speeds associated with the equations depend on the partial derivatives of the pressure, either P_ρ and P_ϵ or P_ρ and P_T. The corresponding expresions are:

$$c = \sqrt{P_\rho + \frac{PP_\epsilon}{\rho^2}} \tag{5}$$

or

$$c = \sqrt{P_\rho + \frac{T(P_T)^2}{c_v \rho^2}} \tag{6}$$

We consider a level set function ϕ, that satisfies

$$(\rho\phi)_t + (\rho u \phi)_x = 0. \tag{7}$$

and this level set equation is coupled to the Euler equations.
We will use two-component Riemann problems as a tool to validate the 1D algorithm of the form:

$$(\rho(x), q(x), P(x), \gamma(x)) = \begin{cases} (\rho_1, q_1, P_1, \gamma_1), & \text{if } x < 0.5 \\ (\rho_2, q_2, P_2, \gamma_2), & \text{if } x \geq 0.5. \end{cases} \tag{8}$$

where $\phi(x) = -1$ if $x < 0.5$, and $\phi(x) = 1$ if $x \geq 0.5$.
We will also use shock-contact problems. A shock-contact problem is an interface between two gases, with different adiabatic exponents, in mechanical, (velocity zero), and thermodynamical (constant pressure at both sides), equilibrium, together with a single shock propagating to the contact. We perform various 1D and 2D experiments using high order accurate reconstruction procedures, including PHM and WENO5. We present a wide validation of our algorithm by performing various numerical one-dimensional experiments with two-component Riemann problems and Shock-Contact Riemann problems for which an exact solution is known. We also consider different accoustic impedances near the contact to validate the algorithm analyzing the type of reflected wave, either a shock wave or a rarefaction wave, when a shock wave hits the interface. We compare the behavior of our algorithm with previous experiments appearing in the literature, remarking the advantages and disadvantages.

We address a 2D simulation of the Richtmyer-Meshkov instability generated by a shock wave impinging a Helium-Air interface in mechanical and thermodynamical equilibrium. We will also study the shock-bubble interaction of a Helium cylindrical bubble in air with a Mach 1.22 shock wave, originally studied by Haas and Sturtevant, ([5]), and addressed by Quirk and Karni in ([6]), from the computational point of view by using a primitive nonconservative second order algorithm. We compare our numerical results with the Haas-Sturtevant experimental data, and getting good agreement with the Haas-Sturtevant data for a simulation performed with our flux-split algorithm together with the WENO5 spatial reconstruction and the third-order accurate Runge-Kutta integration in time, due to Shu and Osher.

References

[1] R. Donat and A. Marquina, *Capturing shock reflections: An improved flux formula*, J. Comp. Phys. **125** (1996), 42-58.

[2] S. Karni, *Multicomponent Flow Calculations by a Consistent Primitive Algorithm* , J. Comp. Phys. **112** (1994), 31-43.

[3] W. Mulder, S. J. Osher and J. Sethian, *Computing Interface Motion in Compressible Gas Dynamics*, J. Comp. Phys., vol.100, pp. 209-228 (1992).

[4] R. P. Fedkiw, T. Aslam and B. Merriman and S. J. Osher, *An Eulerian approach to Interfaces in multimaterial compressible flows, (The Ghost Fluid Method)*, J. Comp. Phys., vol. 152, pp. 452-492 (1999).

[5] J.-F. Haas and B. Sturtevant, *Interaction of weak shock waves with cylindrical and spherical gas inhomogeneities*, J. Fluid. Mech., vol. 181, pp. 41-76 (1987).

[6] J.J. Quirk and S. Karni, *On the dynamics of a shock-bubble interaction*, J. Fluid. Mech. **318** (1996), p. 129.

Pressure Linearization Method for the Computation of Real Fluids

Marica Pelanti

University of Washington, Seattle, WA, USA

We consider the numerical solution of the Euler equations for fluids governed by a general convex equation of state (EOS). In the one-dimensional case, the Euler system takes the form:

$$q_t + f(q)_x = 0\,, \tag{1a}$$

with

$$q = \begin{pmatrix} \rho \\ m \\ E^{\mathrm{t}} \end{pmatrix}, \qquad f(q) = \begin{pmatrix} m \\ \dfrac{m^2}{\rho} + p \\ \dfrac{m}{\rho}(E^{\mathrm{t}} + p) \end{pmatrix} \qquad \text{and} \qquad E^{\mathrm{t}} = E + \frac{m^2}{2\rho}\,. \tag{1b}$$

Here ρ represents the fluid density, $m = \rho u$ the linear momentum, u the velocity along the x-axis, E^{t} the total energy per unit volume, E the internal energy per unit volume, and finally p indicates the pressure. The definition of the problem is completed by providing an equation of state for the fluid, that we assume in the form $p = p(E, \rho)$. Introducing the thermodynamic derivatives associated to $p(E, \rho)$, $\kappa(E, \rho) \equiv \partial p(E, \rho)/\partial E$ and $\chi(E, \rho) \equiv \partial p(E, \rho)/\partial \rho$, we can express the speed of sound of the fluid as $c = \sqrt{\kappa h + \chi}$, where $h = (E + p)/\rho$ is the specific enthalpy.
We propose here a method with the purpose, analogous to the idea in [1], of defining a general and simple procedure for solving the Euler equations for a real fluid by a finite volume method. Our efforts are directed to the formulation of schemes valid for a general equation of state that are as robust and accurate as many classical methods for ideal polytropic gases. In the evolution step, the idea is to replace the original pressure law with a locally-parameterized one, linear in the chosen thermodynamic variables. Then, the original EOS is used in the projection step to define the updated cell-averaged values of the pressure.
Let us introduce a pressure law linear in the selected thermodynamic variables E, ρ in the form

$$p^{\mathrm{L}} = \frac{1}{\psi}(E + \eta\rho + \mu) = p^{\mathrm{L}}(E, \psi, \eta\rho, \mu)\,, \tag{2}$$

where the parameters ψ, η, μ are locally defined. More specifically, given a discretization of the computational domain indexed in space by $i \in \mathbb{Z}$ and in time by $n \in \mathbb{N}$, first we set

$$\bar{\kappa}_i^n = \kappa(E_i^n, \rho_i^n) \qquad \text{and} \qquad \bar{\chi}_i^n = \chi(E_i^n, \rho_i^n)\,, \quad \forall i, n\,, \tag{3}$$

based on the thermodynamic derivatives κ and χ introduced before, and then we define

$$\psi_i^n = \frac{1}{\bar{\kappa}_i^n} \qquad \text{and} \qquad \eta_i^n = \frac{\bar{\chi}_i^n}{\bar{\kappa}_i^n}\,. \tag{4}$$

Since in each cell of the computational domain the consistency condition

$$p(E_i^n, \rho_i^n) = p^{\text{L}}(E_i^n, \psi_i^n, (\eta\rho)_i^n, \mu_i^n) \tag{5}$$

must hold, we then determine uniquely μ_i^n as

$$\mu_i^n = \psi_i^n\, p(E_i^n, \rho_i^n) - E_i^n - (\eta\rho)_i^n\,. \tag{6}$$

The above definition of the parameters ψ, η, μ ensures that the speed of sound we define in each cell through the linear pressure law is the same we would have from the original EOS. This provides an optimal approximation of the speed of the acoustic waves.
The system we solve to approximate the original one consists in the Euler equations with the linear pressure law p^{L}, together with three equations for ψ, $\eta\rho$ and μ, that here are considered as additional variables. We write these supplementary equations governing ψ, $\eta\rho$ and μ by following some approaches [4, 5] proposed in the context of multifluid flow formulations, due to the similarity of the problems. The new system takes the form:

$$q_t + g(q, \psi, \eta\rho, \mu)_x = 0\,, \tag{7a}$$

$$(\eta\rho)_t + (\eta\rho u)_x = 0\,, \tag{7b}$$

$$\psi_t + u\psi_x = 0\,, \tag{7c}$$

$$\mu_t + u\mu_x = 0\,, \tag{7d}$$

where

$$g(q, \psi, \eta\rho, \mu) = \begin{pmatrix} m \\ \dfrac{m^2}{\rho} + p^{\text{L}} \\ \dfrac{m}{\rho}(E^{\text{t}} + p^{\text{L}}) \end{pmatrix}\,, \tag{7e}$$

with p^{L} as in (2).
The proposed algorithm consists then in the following steps:

$i.$ Given q^n, we compute ψ^n, $(\eta\rho)^n$ and μ^n by using the local values of the thermodynamic derivatives and the consistency condition, as in (4), (6). With these initial values at time t^n we solve the new system (7) by a given finite volume method to obtain the updated vector q^{n+1}.

$ii.$ We update the pressure through the original equation of state:

$$p^{n+1} = p(E^{n+1}, \rho^{n+1})\,. \tag{8}$$

Note that, since in (ii) we just need the updated values of the vector $q = (\rho, m, E^{\text{t}})^{\text{T}}$, and not those of the other variables, we don't have to track ψ, $\eta\rho$ and μ, that are instead reset each time step through the relations (4), (6). Thus, in the implementation of our method, we can work with vectors with the same dimension as q, that is with a number of components equal to the number of equations of the original Euler system. The effect of the supplementary equations for ψ, $\eta\rho$ and μ in the scheme is the creation of additional waves, propagating at speed u, that have a role in the updating of the vector q.
The method we have presented defines a simple and general procedure that can be applied to some classical finite volume methods designed for a restricted class of equations of state in order to develop schemes of noticeable flexibility in using different pressure laws. Note also that our method allows to preserve the property of exactly resolving steady contact discontinuities,

since for a problem consisting of a single contact discontinuity the quantities ψ, η and μ are simply advected at the speed of the discontinuity.
In particular, we have specialized our approach to the Roe method [3], and we have performed several numerical tests, both in one and two dimensions. The numerical experimentation proves the flexibility and effectiveness of the method.
It is also worth noticing that the basic formulation of our scheme can be interpreted as a relaxation method, this providing a formal mathematical validation of our approach. From this point of view we find similarity with the *energy relaxation* theory of Coquel and Perthame [1].
We finally remark that it is our hope that the proposed approach will be found useful in developing schemes for the computation of real multicomponent flows, which is the subject of current investigation.

References

[1] F. COQUEL AND B. PERTHAME, Relaxation of Energy and Approximate Riemann Solvers for General Pressure Laws in Fluid Dynamics, *SIAM J. Numer. Anal.*, **35** (1998), 2223–2249.

[2] R. MENIKOFF AND B. J. PLOHR, The Riemann problem for fluid flow of real materials, *Rev. Modern Phy.*, **61** (1989), 75–130.

[3] P. L. ROE, Approximate Riemann Solvers, Parameter Vectors and Difference Schemes, *J. Comput. Phys.*, **43** (1981), 357–372.

[4] R. SAUREL AND R. ABGRALL, A Simple Method for Compressible Multifluid Flows, *SIAM J. Sci. Comput.*, **21** (1999), 1115–1145.

[5] K. M. SHYUE, An Efficient Shock-Capturing Algorithm for Compressible Multicomponent Problems, *J. Comput. Phys.*, **142** (1998), 208–242.

Data Assimilation for Hyperbolic Problem

Rima Gandlin

Weizmann Institute of Science

Multigrid methods are proven to be extremely efficient in the solution of discretized elliptic partial differential equations. However, the attempts to apply the same techniques to non-elliptic problems may lead to a total loss of efficiency in the standard multigrid solver. Usually there are a number of difficulties which increase the amount of required work. Therefore it's important to isolate those difficulties and to analyze them.
Here we consider one of the most important today's problems - *data assimilation*. The current assimilation methods are not only very slow but they are also based on highly questionable compromises such as:
a). assimilating only the data from one time interval at a time without fully correlating
with other intervals;
b). limiting control to only the initial value of the flow at some arbitrary chosen initial
time instead of controlling the numerical equations at all times.
Therefore the purpose is to develop fast multiscale algorithms which can avoid such compromises and can assimilate the data into the multiscale solver of the direct problem at small extra cost.
An example of data assimilation problems is weather prediction. The major problem there is the need to assimilate into the solution of the atmospheric flow equations a continuously incoming stream of data from measurements carried out around the globe with different levels of accurancy, frequency and resolution.

Current assimilation methods require much more computer time and space than the direct solving of atmospheric flow equations. The main reason for this is that any measurement at any place and time should in principle affect the solution at any other place and time, which creates a huge dense matrix of influence.

The fast multiscale algorithm can assimilate the data at a cost comparable to that of solving the direct problem because of three main reasons:

a). large-scale averages may be assimilated well enough on the coarser levels of the multiscale solver, which is not expensive;

b). the correlation of averages on the finer levels is nearly *local*, so that the assimilation at finer levels is local also;

c). the measurements are usually less accurate than the numerical flow itself. Therefore there is no need in doing assimilation at the finest level.

In most current data assimilation approaches, the control parameters, i.e. those changed to obtain fitness of the solution to the data, are only the initial values of the solution. This makes it impossible to benefit from the details (the oscillating components) of the measurements far in time from the initial time because those details at those times are ill-determined by the initial solution, due to the fact that their phase error becomes practically random, in which case the amplitude of the entire solution which would best fit the data can be shown to tend to zero. Therefore, instead of controlling just initial values, i.e. solving *initial control problem* $\underline{(ICP)}$, it is better to control the *entire numerical solution* $\vec{u}$. We call this approach the *residual control problem* $\underline{(RCP)}$. Those control parameters can be effectively handled only by a *Multiscale treatment*.

Our first step was to investigate and compare the two approaches mentioned above in the terms of Fourier components.

As a simple model problem for data assimilation with underlying hyperbolic time-dependent partial differential equation we consider the one dimensional wave equation, where the model is only approximately known and lacks initial conditions, but instead various observations on the solution are given.

In more details, consider

$$u_{tt} = c\triangle u \quad in \;\; \Omega \times [0,T], \quad T \in R^+, \quad \Omega \subset R$$

$$u|_{\partial\Omega} = p(t),$$

$$u|_{t=0} = u_0(x),$$

$$u_t|_{t=0} = g(x),$$

except that part of the model, e.g. some of the functions $c(x,t)$, $u_0(x)$, $g(x)$, $p(t)$, are not known or known only partially, and instead finitely many data $d_j^k \in R$ at points $(x_j, t_k) \in \Omega \times [0,T]$ are given, such that

$$Pu(x_j, t_k) = d_j^k,$$

and define an index set $I = \{(k,j)$, s.t. d_j^k is given$\}$. The projection P represents some local averaging.

The first (and the usual) way of looking at this problem is to solve ICP, i.e. to find an initial function $u_0(x)$ so that the resulting solution $u(x,t)$ of the wave equation would fit the data as well as possible, in the sense of minimizing the functional

$$F(u_0) = \sum_{(k,j)\in I} \beta_j^k \left[Pu(x_j,t_k) - d_j^k \right]^2,$$

where $(\beta_j^k)^{-1}$ is an estimate of the expected square error in the measurements.

The ICP is *ill-posed* in the sense that there is no unique solution depending continuously on the data. There are additional sources of error:

a). discretization and algebraic errors;

b). data noise;

c). modelization errors (the model doesn't describe exactly the real nature's problem).

One way to overcome the ill-posedness is to apply classical regularization technique. The detailed description of an algorithm for solving the ICP stated above using *Tikhonov regularization* can be found in the literature. The analysis of this formulation in terms of Fourier components we present here.

The approach of the *residual control problem* (RCP), on the other hand, involves minimizing the functional

$$F(\vec{u}) = \int_{\Omega\times[0,T]} \gamma R^2 dx dt + \int_{\partial\Omega} \overline{\gamma} R_1^2 dx + \int_0^T \overline{\overline{\gamma}} R_2^2 dt + \sum_{(k,j)\in I} \beta_j^k \left[Pu(x_j,t_k) - d_j^k \right]^2,$$

where γ, $\overline{\gamma}$, $\overline{\overline{\gamma}}$ are weight functions of x, t, u; $R = u_{tt} - \triangle u$ are the residuals of the interior equations; R_1 and R_2 are residuals of the boundary and initial conditions respectively.
The control parameters R, R_1 and R_2 need not be controlled at the finest levels. There they can simply be interpolated from the coarser levels and kept unchanged. Thus, using the method described above, the solution is expected not to be expensive. The Fourier analysis for this method is reported.
Before solving the problem numerically one should choose a suitable discretization scheme. Let h be a meshsize in x-direction and δt be a time step with $K+1$ gridpoints in time-direction, $K\delta t = T$.
The discretization of the Laplacian at time $k\delta t$ is as follows:

$$\triangle^h u_j^k = \frac{u_{j+1}^k - 2u_j^k + u_{j-1}^k}{h^2}.$$

Consider the following second order discretizaion scheme:

$$q\triangle^h u^{k+1} + (1-2q)\triangle^h u^k + q\triangle^h u^{k-1} = \frac{u_j^{k+1} - 2u_j^k + u_j^{k-1}}{\delta t^2},$$

where $0 \le q \le 1$ is a parameter, which has to be determined.
In order to find q such that this discretization scheme would be unconditionally stable we also apply the Fourier analysis.
The two methods - $\underline{RCP}$ and $\underline{ICP}$ are compared in terms of Fourier components. Then a minimization problem for *RCP* is formulated. The main future goal is to develop a fast multigrid algorithm for this problem.

4.21 Tuesday, Session 5 (morning): Kinetics

Kinetic schemes for relativistic gas dynamics

M. Kunik, S. Qamar and G. Warnecke*

Institut fuer Analysis und Numerik, Otto-von-Guericke-Universitaet Magdeburg, PSF 4120, D-39016 Magdeburg, Germany

A kinetic scheme for the relativistic Euler equations is presented. These equations describe the flow of the particle density, the spatial part of the four-velocity and pressure. The non-relativistic and ultra-relativistic limits are covered. The scheme consists of a free flight time step coupled with an equilibration using Juettner's relativistic generalization of the classical Maxwellian phase density. Some properties of the scheme such as conservation of mass, momentum and entropy as well as an entropy inequality are shown. Also some simple computations are presented.

Design of numerically efficient kinetic models

Hans Babovsky

Ilmenau Technical University, Germany

1. Introduction. Discrete kinetic models for the numerical simulation of nonlinear kinetic equations (in particular the Boltzmann equation) may be obtained from the discretization of the original Boltzmann collision operator. There are a couple of research groups having made proposals in this direction (e.g. [7, 8, 9, 10, 11, 13] to mention some of the publications of recent years). Although many attempts have been made to design efficient numerical schemes the question of solving kinetic equations in a realistic setting is still a very challenging task – in particular if one keeps in mind the transition regime close to the fluid dynamic limit, where kinetic equations become extremely stiff and thus very expensive to solve.

The main obstacle against an efficient solver for the Boltzmann operator is the collision integral which contains an in general five-dimensional integral which has to be evaluated at each time step in each point of the (discretized) six-dimensional phase space. On the other hand, close to the fluid dynamic limit too detailed descriptions of the collision kernel are not really useful. The main ingredients for a reasonable discrete model are the conservation laws and certain integral quantities to ensure the correct flow coefficients. For this reason, simplified relaxation models have been proposed, in particular extensions of the well-known BGK model (e.g. the ES-BGK model as treated in [2]). While such schemes seem to be well-adapted to simulate the transition to fluid dynamics, they bar the way back to more rarefied regimes, since one main feature of gas kinetics has been given up – the two-particle collision interaction. For this reason, such models in our opinion do not allow to really understand what is going on when passing from rarefied flows to continuum flows. There are alternative approaches for the transition, like minimum entropy principles, to cut down the infinite moment hierarchy to a finite system; these are applied e.g. in Extended Thermodynamics [12], but they rely as well on phenomenological arguments. On the other hand, Domain Decomposition techniques do not seem to be a tool as powerful as expected by a number of scientists in the 1990'.

2. Requirements for useful kinetic schemes. The discrete kinetic schemes we have in mind must balance the requirements of reduced complexity (which seems to be necessary for numerical efficiency) and of physical principles. Our intention are models which (at least in specific situations) are capable of covering the whole spectrum between extremely rarefied gases (Knudsen gas) to the fluid dynamic limit. In particular, these requirements are:

(i) The model should be based on reversible moment preserving two particle collisions; this ensures immediately the conservation of mass, momentum and kinetic energy, and the H-Theorem; it does not guarantee that there are no additional artificial conservation laws. Measures have to be taken to exclude these. The model should be flexible enough that collision frequencies may be adjusted to yield the correct fluid flow parameters.

(ii) The collision operator must have a numerically efficient ”fast” solver; one should be able to exploit the structure in a parallel computer environment. Stiffness problems must be reduced by an efficient handling of collision parameters which is to be implemented in an adaptive scheme.

(iii) There must be a strategy to pass over gradually from rarefied regimes to the fluid dynamic limit. This may be obtained by a hierarchical collision model with small scale and large scale structures.

3. Design of kinetic models. The first feature of our artificial discrete systems is based on the observation that special collision systems with parameters which are defined according to a partition of a rectangular grid give rise to a hierarchical system of kinetic equations. Properly transformated, this system decouples a small part of nonlinear equations from a large linear one. The study of the linearized equations demonstrates that the linear operator may be decomposed in a way which reduces the number of required operations impressively (very much like the decomposition of the discrete Fourier transformation leads to the Fast Fourier Transformation). This decomposition rule can be carried over to the nonlinear equations. This model has first been proposed in [3] and is also described in [5, 6]. It is a preliminary model which due to the restriction to ”axiparallel” collision laws has artificial collision invariants which have to be suppressed by appropriate projection methods. This feature can be readily removed by using rotating grids (in velocity space). On the other hand, the projections can be handled such that the fluid dynamic limit results in the correct Euler equations.

Based on the model above, a system of more and more refining multilevel structures in velocity space can be constructed (resembling a Haar wavelet decomposition of the velocity space). This system keeps all the desirable properties of the one-level scheme described above. One way to pass to the fluid dynamic limit is to speed up the small scale collision procedure up to a certain level, thus reducing the number of flow variables. This reduction can be done adaptively in a fluid domain thus establishing a ”smooth” transition from gas kinetics to fluid dynamics. Such a scheme has been proposed in [4] (see also [5]). A more sophisticated and flexible model with the correct number of collision invariants is presently to be constructed [1].

4. Conclusions. We are going to give impulses for the design of discrete kinetic models which combine a large amount of complexity as given in the models of Rarefied Gas Dynamics with efficient solvability and which allow for a hierarchical structure which makes it possible to study in detail questions concerning the passage to the fluid dynamic limit.

References

[1] L. S. Andallah and H. Babovsky. (In preparation)

[2] P. Andries, J.F. Bourgat, P. Le Tallec, B. Perthame. *Numerical comparison between the Boltzmann and ESBGK models for rarefied gases.* Preprint no. 3872, INRIA Rocquencourt, 2000.

[3] H. Babovsky. *Reducible kinetic equations.* Preprint M 20/00, Inst. f. Mathematik, TU Ilmenau, 2000 (zur Veröffentlichung eingereicht).

[4] H. Babovsky. *A kinetic multiscale model.* Preprint M 24/00, Inst. f. Mathematik, TU Ilmenau, 2000 (to appear in M 3 AS).

[5] H. Babovsky. *Hierarchies of reducible kinetic models*, in: Discrete Modelling and Discrete Algorithms in Continuum Mechanics, Th. Sonar and I. Thomas (Eds.), Logos Verlag, Berlin 2001.

[6] H. Babovsky, D. Görsch and F. Schilder, Steady kinetic boundary value problems. Preprint M 01/02, Inst. f. Mathematik, TU Ilmenau, 2002 (to appear).

[7] A.V. Bobylev, A. Palczewski and J. Schneider. *On the approximation of the Boltzmann equation by discrete velocity models.* C. R. Acad. Sci. Paris I 320(5):639–644, 1995.

[8] A. V. Bobylev and S. Rjasanow. *Fast deterministic method of solving the Boltzmann equation for hard spheres.* European J. Mech. B Fluids, 18:869–887, 1999.

[9] A. V. Bobylev and S. Rjasanow. *Numerical solution of the Boltzmann Equation using a fully conservative difference scheme based on the Fast Fourier Transform.* Transport Theor. Stat. Phys., 29:289–310, 2000.